Inorganic Chemistry

Article

pubs.acs.org/IC

Efficient Synthesis of Tris-Heteroleptic Iridium(III) Complexes Based on the Zn^{2+}-Promoted Degradation of Tris-Cyclometalated Iridium(III) Complexes and Their Photophysical Properties

Yuichi Tamura,[†] Yosuke Hisamatsu,[†] Sarvendra Kumar,[†] Taiki Itoh,[†] Kyouhei Sato,[‡] Reiko Kuroda,[‡] and Shin Aoki*[,†,§,∥]

[†]Faculty of Pharmaceutical Science and [§]Division of Medical-Science-Engineering Cooperation, [∥]Imaging Frontier Center, [‡]Research Institute for Science and Technology, Tokyo University of Science, 2641 Yamazaki, Noda, Chiba 278-8510, Japan

Supporting Information

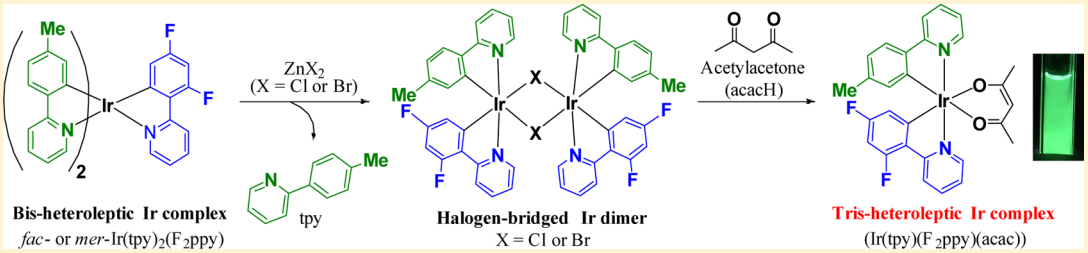

ABSTRACT: We report on the efficient synthesis of tris-heteroleptic iridium (Ir) complexes based on the degradation of tris-cyclometalated Ir complexes (IrL_3, L: cyclometalating ligand) in the presence of Brønsted and Lewis acids such as HCl (in 1,4-dioxane), $AlCl_3$, TMSCl, and ZnX_2 (X = Br or Cl), which affords the corresponding halogen-bridged Ir dimers (μ-complexes). Tris-cyclometalated Ir complexes containing electron-withdrawing groups such as fluorine, nitro, or CF_3 moieties on the ligands were less reactive. This different reactivity was applied to the selective degradation of heteroleptic Ir complexes such as *fac*-Ir(tpy)$_2$(F$_2$ppy) (***fac*-12**) (tpy: 2-(4′-tolyl)pyridine and F$_2$ppy: 2-(4′,6′-difluorophenyl)pyridine), *mer*-Ir(tpy)$_2$(F$_2$ppy) (***mer*-12**), and *mer*-Ir(mpiq)$_2$(F$_2$ppy) (***mer*-15**) (mpiq: 1-(4′-methylphenyl)isoquinoline). For example, the reaction of ***mer*-12** with $ZnBr_2$ gave the heteroleptic μ-complex [{Ir(tpy)(F$_2$ppy)(μ-Br)}$_2$] **27b** as a major product, resulting from the selective elimination of the tpy ligand of ***mer*-12**, and treatment of **27b** with acetylacetone (acacH) afforded the corresponding tris-heteroleptic Ir complex Ir(tpy)(F$_2$ppy)(acac)**18**. In addition, another tris-heteroleptic Ir complex **35a** having 8-benzenesulfonylamidoquinoline (8BSQ) ligand was synthesized. Mechanistic studies of this degradation reaction and the photochemical properties, especially a dual emission, of these newly synthesized tris-heteroleptic Ir complexes are also reported.

INTRODUCTION

Cyclometalated iridium(III) (Ir(III)) complexes have received considerable attention as phosphorescent emitters[1] and have been applied in broad research areas related to organic light emitting diodes (OLEDs),[2] bioimaging probes,[3] oxygen sensors,[4] anticancer agents,[5] photoredox catalysts,[6] pH sensors,[7] and so on.[8] Over the past decade, the preparation of numerous Ir complexes by ligand functionalization, most of which can be classified into IrL_3, IrL_2L', and IrL_2A (where L and L′ are different cyclometalating ligands and A is an ancillary ligand), have been reported. However, the efficient synthesis and photophysical properties of tris-heteroleptic Ir complexes represented by IrLL′A are yet to be studied.

As shown in Chart 1, the synthesis of tris-heteroleptic Ir complexes (IrLL′A) is typically carried out by the reaction of a chloro-bridged dimer, prepared from $IrCl_3$ and two different cyclometalating ligands (L and L′), with a corresponding ancillary ligand (A).[9] This method gives a mixture of IrLL′A with IrL_2A and IrL'_2A, making their purification difficult, which usually results in low chemical yields. Because the reactions of heteroleptic μ-complexes with nonsymmetric ancillary ligands provide its diastereomers,[9a,b,f] examples of isolated tris-heteroleptic Ir complexes (a mixture of enantiomers (Δ and Λ forms)) have been limited to compounds that contain symmetric ancillary ligands.[9c−g] Baranoff and co-workers have recently reported on the synthesis of the tris-heteroleptic Ir complex, Ir(ppy)(F$_2$ppy)(acac) (ppy 2-phenylpyridine, F$_2$ppy 2-(4′,6′-difluorophenyl)pyridine, and acac acetylacetonate), by reacting an Ir complex [{Ir(COD)(μ-Cl)}$_2$] with ppy and F$_2$ppy ligands.[9d,e] Moreover, they reported that the degradation of Ir(ppy)(F$_2$ppy)(acac) induced by HCl (2 M in Et$_2$O) provided a heteroleptic μ-complex [{Ir(ppy)(F$_2$ppy)(μ-Cl)}$_2$], which is a useful intermediate for the synthesis of other tris-heteroleptic Ir complexes containing ppy and F$_2$ppy ligands. Although this method is also accompanied by burdensome purification and low product yields, it is the only reported method to date for preparing tris-heteroleptic Ir complexes.

Received: September 21, 2016

DOI: 10.1021/acs.inorgchem.6b02270
Inorg. Chem. XXXX, XXX, XXX−XXX

Chart 1

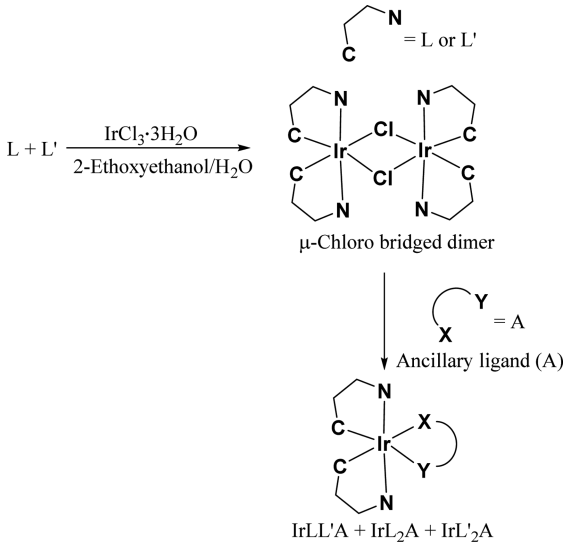

We previously reported on regioselective substitution reactions (e.g.; halogenations, nitration, and Vilsmeier−Haack formylation) of *fac*-tris-homoleptic cyclometalated Ir complexes, *fac*-Ir(ppy)$_3$ (***fac*-1**), (ppy 2-phenylpridine), *fac*-Ir(tpy)$_3$ (***fac*-2**) (tpy 2-(4′-tolyl)pyridine), and *fac*-Ir(mppy)$_3$ (***fac*-3**) (mppy 2-(4′-methoxyphenyl)pyridine), at the 5′-position (the *p*-position with respect to the C−Ir bond) on 2-phenylpyridine ligands and their subsequent conversions to produce **4** containing a variety of functional groups (Chart 2).[10,11]

Chart 2

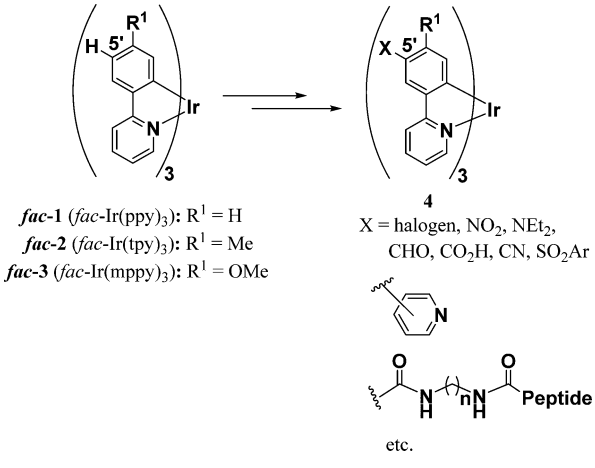

These findings allowed us to design and synthesize pH-responsive Ir complexes that contain basic groups,[10a,11a,c,d] blue-colored Ir complexes,[10b] and amphiphilic Ir complexes containing cationic peptides that have cytotoxic activity against cancer cells.[11b,e]

During these experiments, it was found that the reaction of ***fac*-2** with acetyl chloride in the presence of $AlCl_3$ (Friedel−Crafts acylation conditions) afforded the chloro-bridged Ir dimer **6a** in 68% yield, and not an acetyl derivative **5** (Chart 3).[10a] This finding prompted us to examine the reactions of tris-cyclometalated Ir complexes with a variety of Lewis acids.

In this manuscript, we report that Lewis acids such as zinc halides (ZnX_2), $AlCl_3$, and TMSCl promote the degradation of tris-cyclometalated homoleptic Ir complexes including *fac*-

Chart 3

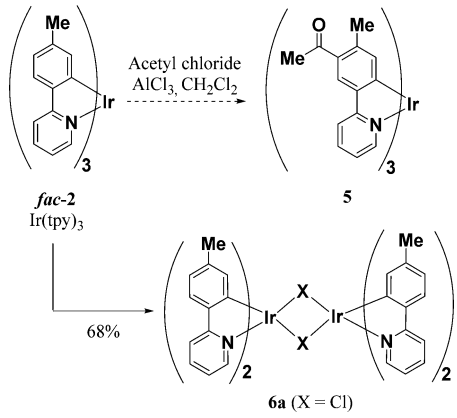

Ir(ppy)$_3$ (***fac*-1**), *mer*-Ir(ppy)$_3$ (***mer*-1**), *fac*-Ir(tpy)$_3$ (***fac*-2**), *mer*-Ir(tpy)$_3$ (***mer*-2**), *fac*-Ir(mppy)$_3$ (***fac*-3**), *fac*-Ir(Br-tpy)$_3$ (***fac*-7**) (Br-tpy 2-(5′-bromo-4′-tolyl)pyridine), *fac*-Ir(mpiq)$_3$ (***fac*-10**) (mpiq 1-(4′-methylphenyl)isoquinoline), and *mer*-Ir(mpiq)$_3$ (***mer*-10**) to provide the corresponding halogen-bridged Ir dimers (μ-complexes) such as **6a** from ***fac*-** and ***mer*-2** (Charts 4 and 5). In contrast, tris-cyclometalated Ir

Chart 4

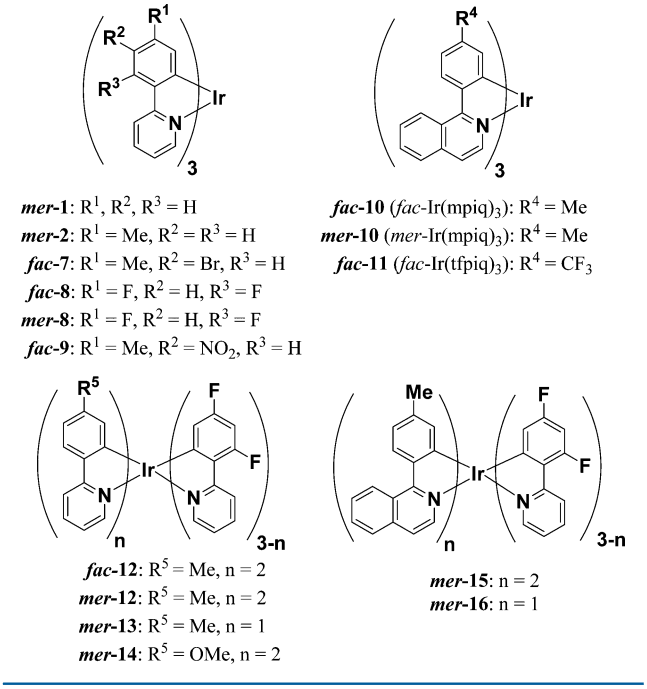

complexes that contain cyclometalated ligands containing an electron-withdrawing group such as *fac*-Ir(F$_2$ppy)$_3$ (***fac*-8**), *fac*-Ir(tpy-NO$_2$)$_3$ (***fac*-9**) (tpy-NO$_2$ 2-(5′-nitro-4′-tolyl)pyridine), and *fac*-Ir(tfpiq)$_3$ (***fac*-11**) (tfpiq 1-(4′-trifluoromethylphenyl)-isoquinoline) were less reactive. The μ-complex **6a** was reacted with acetylacetone (acacH) to afford Ir(tpy)$_2$(acac) **17** (Chart 5). Because these types of Ir complexes that contain two identical ligands are readily available (for example, **17** can be synthesized from tpy via **6a**), we examined the ligand-selective degradation reactions of tris-cyclometalated heteroleptic Ir complexes, ***fac*-12** and ***mer*-12-16**, containing two different ligands such as tpy, mppy, mpiq, and F$_2$ppy (Chart 4), in the presence of Brønsted and Lewis acids. As a result, it was found

DOI: 10.1021/acs.inorgchem.6b02270
Inorg. Chem. XXXX, XXX, XXX−XXX

Chart 5

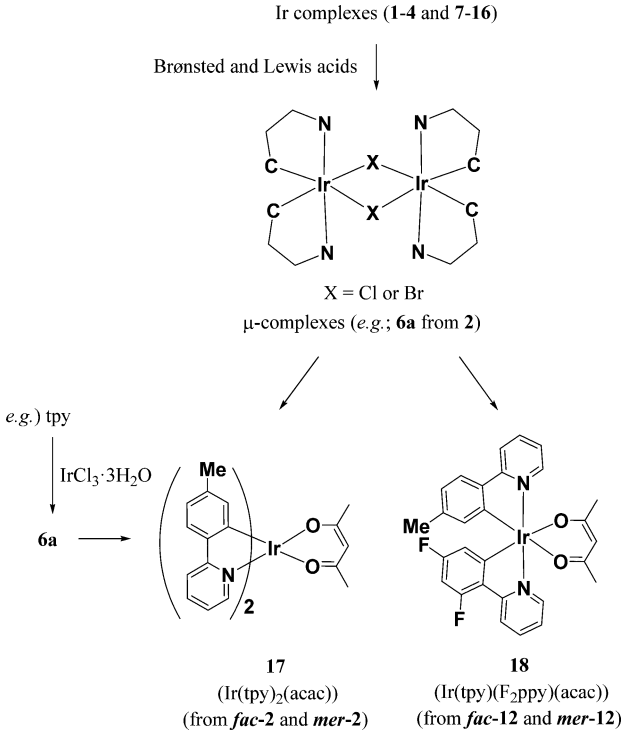

that the reaction of ***fac*-12** with $ZnBr_2$ gives the heteroleptic μ-complex $[\{Ir(tpy)(F_2ppy)(\mu\text{-}Br)\}_2]$ as the major product due to the selective elimination of its tpy ligand and the product, on reaction with acetylacetone (acacH), afforded the tris-heteroleptic Ir complex Ir(tpy)(F_2ppy)(acac) **18** (Chart 5). Moreover, novel tris-heteroleptic Ir complexes containing an ancillary ligand (e.g.; 8-benzenesulfonylamidoquinoline (8BSQ)) were obtained. Mechanistic studies of this degradation reaction and photochemical properties of these newly synthesized tris-heteroleptic Ir complexes are also described.[12]

EXPERIMENTAL PROCEDURES

General Information. $IrCl_3{\cdot}3H_2O$ was purchased from KANTO CHEMICAL Co. Glycerol and AgOTf was purchased from NACALAI TESQUE, INC. Anhydrous 1,2-dichloroethane was obtained by distillation from calcium hydride and 1,2-dichloroethane-d_4 was purchased from SIGMA-Aldrich. ^{1}H NMR spectra (300 and 400 MHz) were recorded on a JEOL Always 300 spectrometer and a JEOL Lambda 400 spectrometer, and IR spectra were recorded on a PerkinElmer FTIR Spectrum 100 (ATR). Electrospray ionization (ESI) mass spectra were recorded on a Varian 910-MS spectrometer. Thin-layer chromatographies (TLC) and silica gel column chromatographies were performed using Merck 5554 (silica gel) TLC plates and Fuji Silysia Chemical FL-100D, respectively. Emission lifetimes were determined using a TSP-1000 spectrometer (Unisoku Co., Ltd.). Commercially available DMSO (spectrophotometric grade, WAKO CHEMICAL Co.) was used for the measurement of photophysical data. Elemental analyses of the Ir complexes, except for ***mer*-10** and **36** were not carried out because the metal and/or halogen contents of these compounds are >25%. Density functional theory (DFT) calculations were also carried out using the Gaussian09 program[13] (B3LYP, the LanL2DZ basis set for a Ir and Br atoms and the 6-31G basis set for H, C, F, S, O, N atoms).[14] Time-dependent DFT (TD-DFT) calculations were carried out based on all the ground state geometries. The chromaticity values obtained from emission spectra of Ir complexes were plotted on a color diagram using a ColorAC software.

Synthesis. The compounds ***fac*-1**,[1h,15] ***mer*-1**,[1h] ***fac*-2**,[1h,10a] ***mer*-2**,[1h] ***fac*-3**,[10b] ***mer*-3**,[1h] ***fac*-7**,[10a] ***fac*-8**,[1h,15] ***mer*-8**,[1h] ***fac*-9**,[10a] ***fac*-10**,[11a] ***fac*-11**,[11a] **17**,[16] and **22b**[16] were prepared in the form of a racemic mixture of Λ and Δ forms and their spectral data were in good agreement with reported data.

*$[\{Ir(tpy)_2(\mu\text{-}Br)\}_2]$ (**6b**).*[17] A solution of ***fac*-2** (30 mg, 43 μmol) and $ZnBr_2$ (0.50 g, 2.2 mmol) in 1,2-dichloroethane (2.0 mL) was refluxed for 3 h. After cooling to room temperature, the insoluble materials were removed by filtration and the filtrate was concentrated under reduced pressure. The crude residue was purified by silica gel column chromatography using $CHCl_3$ as the eluent to give **6b** as a yellow powder (24 mg, 93% yield). mp >300 °C. IR (ATR): ν = 1604, 1587, 1560, 1476, 1462, 1426, 1152, 1065, 769, 747, 664, 427 cm^{-1}. ^{1}H NMR (300 MHz, $CDCl_3/Si(CH_3)_4$) δ = 9.43 (d, J = 5.7 Hz, 4H), 7.82 (d, J = 6.9 Hz, 4H), 7.74 (td, J = 6.9, 1.2 Hz, 4H), 7.36 (d, J = 8.1 Hz, 4H), 6.81 (td, J = 6.3, 1.8 Hz, 4H), 6.55 (d, J = 7.2 Hz, 4H), 5.72 (s, 4H), 1.93 (s, 12H). ESI-MS (m/z). Calcd for $C_{48}H_{40}N_4Br_2Ir_2$ (M^+): 1216.0841. Found: 1216.0841.

*mer-Ir(mpiq)$_3$ (**mer-10**):*[17] A mixture of chloro-bridged Ir dimer $[\{Ir(mpiq)_2(\mu\text{-}Cl)\}_2]$ (**19a**) (prepared from 1-(4′-methylphenyl)-isoquinoline (mpiq) and $IrCl_3{\cdot}3H_2O$ as shown in Chart 6) (0.20 g, 0.18 mmol), K_2CO_3 (0.56 g, 4.0 mmol), and mpiq (0.26 mg, 0.12 mmol) in glycerol (5.0 mL) was stirred at 150 °C for 8 h. After cooling to room temperature, water was added to the reaction mixture and extracted with $CHCl_3$. The combined organic layer was dried over Na_2SO_4 and filtered to obtain the filtrate, to which hexanes and

Chart 6. Synthesis of *fac*-2, *mer*-2, *fac*-10, *mer*-10, *fac*-12, *mer*-12 and *mer*-15

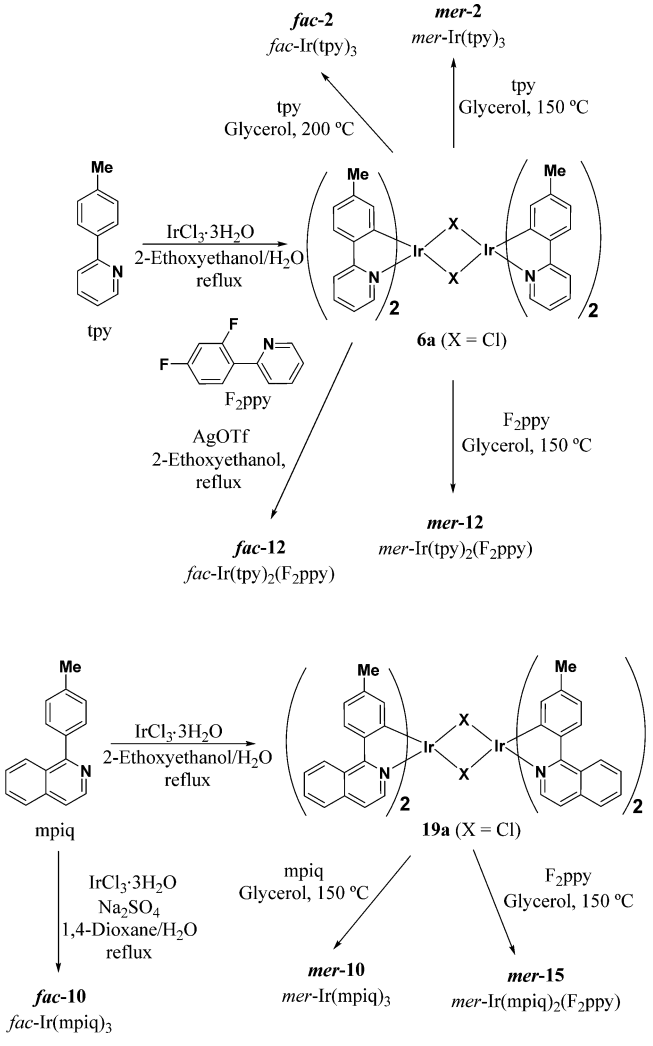

DOI: 10.1021/acs.inorgchem.6b02270
Inorg. Chem. XXXX, XXX, XXX−XXX

CH_2Cl_2 were added to obtain ***mer*-10** as a red powder (0.13 g, 52% yield). mp 219−220 °C. IR (ATR): ν = 2917, 1580, 1499, 1438, 1347, 1311, 1269, 1206, 1146, 1120, 1040, 868, 811, 737, 672, 581, 418 cm^{-1}. ^1H NMR (300 MHz, $CDCl_3/Si(CH_3)_4$) δ = 8.99−8.87 (m, 3H), 8.20 (d, J = 8.4 Hz, 1H), 8.09 (t, J = 6.6 Hz, 3H), 7.70−7.56 (m, 10H), 7.52 (d, J = 6.3 Hz, 1H), 7.10 (d, J = 6.3 Hz, 1H), 6.97 (d, J = 6.9 Hz, 1H), 6.90 (d, J = 6.6 Hz, 1H), 6.85 (d, J = 8.1 Hz, 2H), 6.78 (d, J = 8.7 Hz, 1H), 6.74 (s, 1H), 6.47 (s, 1H), 6.32 (s, 1H), 2.13 (s, 3H), 2.11 (s, 3H), 2.09 (s, 3H). ESI-MS (m/z). Calcd for $C_{48}H_{36}N_3{}^{191}Ir$ (M^+): 845.2510. Found: 845.2514. Anal. Calcd for $C_{48}H_{36}N_3Ir$: C, 68.06; H, 4.28; N, 4.96. Found: C, 67.70; H, 4.19; N, 4.89.

fac-Ir(tpy)$_2$(F$_2$ppy) ***(fac-12)***.[17] A solution of the F_2ppy ligand (0.15 g, 0.76 mmol), the chloro-bridged Ir dimer $[\{Ir(tpy)_2(\mu\text{-}Cl)\}_2]$ **6a**[16] (0.20 g, 0.18 mmol), and AgOTf (90 mg, 0.35 mmol) in 2-ethoxyethanol (3.0 mL) was refluxed for 3 h. The yellow precipitate was filtrated on a filter and dried for 1 h. The combined bright yellow powder was purified by silica gel column chromatography using hexanes/CH_2Cl_2 (2/1) as the eluent to afford ***fac*-12** as a yellow powder (0.12 g, 46% yield). mp >300 °C. IR (ATR): ν = 1597, 1554, 1470, 1397, 1264, 1237, 1159, 1098, 982, 829, 808, 769, 748, 725, 717, 567, 523, 429 cm^{-1}. ^1H NMR (300 MHz, $CDCl_3/Si(CH_3)_4$) δ = 8.26 (d, J = 8.4 Hz, 1H), 7.83 (dd, J = 7.8, 3.3 Hz, 2H), 7.62−7.50 (m, 6H), 7.44 (d, J = 5.4 Hz, 1H), 7.39 (d, J = 5.4 Hz, 1H), 6.88−6.79 (m, 3H), 6.73 (td, J = 7.2, 1.8 Hz, 2H), 6.64 (s, 1H), 6.61 (s, 1H), 6.39−6.30 (m, 2H), 2.17 (s, 3H), 2.12 (s, 3H). ESI-MS (m/z). Calcd for $C_{35}H_{26}N_3F_2{}^{191}Ir$ (M^+): 717.1695. Found: 717.1702.

mer-Ir(tpy)$_2$(F$_2$ppy) ***(mer-12)***.[17] A mixture of **6a** (0.20 g, 0.18 mmol), K_2CO_3 (0.25 g, 1.8 mmol) and the F_2ppy ligand (0.14 g, 0.72 mmol) in glycerol (5.0 mL) was stirred at 150 °C for 24 h. After cooling to room temperature, water was added to the reaction mixture and extracted with $CHCl_3$. The combined organic layer was dried over Na_2SO_4, filtered, and the resulting filtrate was concentrated under reduced pressure and then purified by silica gel column chromatography using hexanes/$CHCl_3$ (2/1) as the eluent to afford ***mer*-12** as a yellow powder (0.19 g, 74% yield). mp >300 °C. IR (ATR): ν = 1588, 1552, 1466, 1420, 1392, 1281, 1262, 1231, 1158, 1095, 1054, 977, 872, 806, 769, 750, 717, 569, 522, 426 cm^{-1}. ^1H NMR (400 MHz, $CDCl_3/Si(CH_3)_4$) δ = 8.29 (d, J = 8.4 Hz, 1H), 8.00 (d, J = 6.0 Hz, 1H), 7.94 (d, J = 5.2 Hz, 1H), 7.75 (d, J = 8.0 Hz, 2H), 7.62−7.46 (m, 6H), 6.88 (t, J = 6.4 Hz, 1H), 6.78−6.68 (m, 4H), 6.39−6.33 (m, 3H), 6.18 (s, 1H), 2.14 (s, 3H), 2.12 (s, 3H). ESI-MS (m/z). Calcd for $C_{35}H_{26}N_3F_2{}^{191}Ir$ (M^+): 717.1695. Found: 717.1696.

mer-Ir(F$_2$ppy)$_2$(tpy) ***(mer-13)***.[17] A mixture of AgOTf (0.32 g, 1.2 mmol), chrolo-bridged Ir dimer $[\{Ir(F_2ppy)_2(\mu\text{-}Cl)\}_2]$[16] (0.30 g, 0.25 mmol), the tpy ligand (0.12 g, 0.75 mmol), and triethylamine (0.14 g, 0.75 mmol) in 1,2-dichloroethane (50 mL) was refluxed for 2 h. The mixture was then cooled to room temperature, and the precipitate was removed by filtration. The filtrate was evaporated under reduced pressure and purified by silica gel column chromatography using $CHCl_3$ as the eluent to afford ***mer*-13** as a yellow powder (0.26 g, 72% yield), mp >300 °C. IR (ATR): ν = 1595, 1564, 1551, 1469, 1397, 1285, 1237, 1157, 1096, 981, 834, 807, 772, 749, 711, 566, 524 cm^{-1}. ^1H NMR (400 MHz, $CDCl_3/Si(CH_3)_4$) δ = 8.21−8.19 (m, 2H), 8.09 (d, J = 5.1 Hz, 1H), 7.89 (d, J = 8.1 Hz, 1H), 7.82 (d, J = 4.8 Hz, 1H), 7.65−7.50 (m, 5H), 6.89 (td, J = 6.0, 1.2 Hz, 1H), 6.83 (dd, J = 7.5, 1.5 Hz, 1H), 6.75 (q, J = 7.5 Hz, 2H), 6.69 (s, 1H), 6.46−6.30 (m, 2H), 5.98 (dd, J = 6.9, 2.1 Hz, 1H), 5.81 (dd, J = 9.6, 2.1 Hz, 1H), 2.17 (s, 3H). ESI-MS (m/z). Calcd for $C_{34}H_{22}N_3F_4{}^{191}Ir$ (M^+): 739.1350. Found: 739.1358.

mer-Ir(mppy)$_2$(F$_2$ppy) ***(mer-14)***.[17] ***mer*-14** was obtained as a yellow powder (67 mg, 17% yield) from $[\{Ir(mppy)_2(\mu\text{-}Cl)\}_2]$[18] (0.30 g, 0.25 mmol), K_2CO_3 (0.35 g, 2.5 mmol), glycerol (15 mL) and F_2ppy ligand (0.14 g, 0.76 mmol) using a precedure similar to that for ***mer*-12**. The product was purified by silica gel column chromatography with $CHCl_3$ as the eluent. mp >300 °C. IR (ATR): ν = 1579, 1508, 1476, 1427, 1399, 1278, 1213, 1158, 1101, 1042, 984, 835, 768, 589, 567, 525, 420 cm^{-1}. ^1H NMR (300 MHz, $CDCl_3/Si(CH_3)_4$) δ = 8.30 (dd, J = 8.1, 2.1 Hz, 1H), 7.98−7.96 (m, 2H), 7.68−7.43 (m, 8H), 6.89 (t, J = 6.9 Hz, 1H), 6.71−6.63 (m, 2H), 6.56−6.34 (m, 4H), 6.10 (d, J = 2.7 Hz, 1H), 5.91 (d, J = 2.7 Hz, 1H), 3.62 (s, 3H), 3.58 (s, 3H). ESI-MS (m/z). Calcd for $C_{35}H_{26}N_3O_2F_2{}^{191}Ir$ (M^+): 749.1593. Found: 749.1578.

mer-Ir(mpiq)$_2$(F$_2$ppy) ***(mer-15)***.[17] ***mer*-15** was prepared as a red powder (0.20 g, 81% yield) from **19a** (0.20 g, 0.15 mmol), K_2CO_3 (0.42 g, 3.0 mmol), glycerol (5 mL), and F_2ppy ligand (0.22 g, 0.90 mmol) using a precedure similar to that for ***mer*-12**. The product was purified by silica gel column chromatography with hexanes/CH_2Cl_2 (2/1) as the eluent. mp 252−253 °C. IR (ATR): ν = 1583, 1554, 1500, 1470, 1440, 1391, 1348, 1264, 1231, 1159, 1148, 1122, 1096, 1043, 978, 867, 810, 751, 737, 717, 672, 579, 567, 522 cm^{-1}. ^1H NMR (300 MHz, $CDCl_3/Si(CH_3)_4$) δ = 8.98−8.89 (m, 2H), 8.31 (d, J = 8.1 Hz, 1H), 8.16 (d, J = 8.4 Hz, 1H), 8.11 (d, J = 8.1 Hz, 1H), 7.95 (d, J = 6.3 Hz, 1H), 7.78−7.73 (m, 3H), 7.66−7.57 (m, 5H) 7.43 (d, J = 6.3 Hz, 1H), 7.07−7.01 (m, 2H), 6.85−6.77 (m, 3H), 6.45−6.24 (m, 4H), 2.09 (s, 3H), 2.08 (s, 3H). ESI-MS (m/z). Calcd for $C_{43}H_{30}N_3F_2{}^{191}Ir$ (M^+): 817.2008. Found: 817.2008.

mer-Ir(F$_2$ppy)$_2$(mpiq) ***(mer-16)***.[17] The chloro-bridged Ir dimer $[\{Ir(F_2ppy)_2(\mu\text{-}Cl)\}_2]$ (0.10 g, 78 μmol), AgOTf (0.10 g, 0.39 mmol), triethylamine (23 mg, 0.24 mmol), the mpiq ligand (52 mg, 0.24 mmol) were reacted in 1,2-dichloroethane (15 mL) using a precedure similar to that for ***mer*-13**. The crude product was purified by silica gel column chromatography with hexanes/$CHCl_3$ (4/1) as the eluent to give ***mer*-16** as an orange powder (60 mg, 48% yield). mp >300 °C. IR (ATR): ν = 1594, 1567, 1552, 1471, 1397, 1286, 1237, 1157, 1112, 1097, 1039, 981, 807, 783, 752, 740, 711, 676, 567, 524, 383 cm^{-1}. ^1H NMR (300 MHz, $CDCl_3/Si(CH_3)_4$) δ = 8.94−8.91 (m, 1H), 8.21−8.19 (m, 2H), 8.10 (d, J = 8.1 Hz, 1H), 8.06 (d, J = 5.7 Hz, 1H), 7.80−7.76 (m, 2H), 7.70−7.63 (m, 2H), 7.56−7.49 (m, 3H), 7.21 (d, J = 5.7 Hz, 1H), 6.90 (dd, J = 7.8, 1.5 Hz, 1H), 6.84 (s, 1H), 6.75−6.65 (m, 2H), 6.48−6.37 (m, 2H), 5.98 (dd, J = 8.1, 2.4 Hz, 1H), 5.81 (dd, J = 8.1, 2.4 Hz, 1H), 2.22 (s, 3H). ESI-MS (m/z). Calcd for $C_{38}H_{24}N_3F_4{}^{191}Ir$ (M^+): 789.1507. Found: 789.1503.

Ir(tpy)(F$_2$ppy)(acac) ***(18)***.[17] A solution of ***mer*-12** (20 mg, 28 μmol) and $ZnBr_2$ (0.31 g, 1.4 mmol) in 1,2-dichloroethane (2.0 mL) was refluxed for 3 h. After cooling to room temperature, the insoluble materials were removed by filtration washing with $CHCl_3$ and the filtrate was concentrated under reduced pressure. The crude product was purified by silica gel column chromatography using $CHCl_3$ as the eluent to give the mixture of **6b** and **27b** (18 mg, quant. assuming that only **27b** was obtained) as a yellow powder.

As reported by Baranoff and co-workers,[9d] a mixture of **6b** and **27b** obtained above (18 mg, 14 μmol), tetrabutylammonium hydroxide (TBAH) (30 mg, 42 μmol) and acetylacetone (6.0 mg, 56 μmol) in CH_2Cl_2/MeOH (10/1, 1.1 mL) was refluxed for 1 h. After cooling to room temperature, water was added to the reaction mixture and the resulting solution was extracted with $CHCl_3$. The combined organic layer was dried over Na_2SO_4. After filtration, the solvent was concentrated under reduced pressure and the resulting residue was purified by silica gel chromatography using hexanes/CH_2Cl_2 (4/1) as the eluent to give **18** as a yellow powder (10 mg, 63% yield from ***mer*-12**). mp >300 °C. IR (ATR): ν = 2923, 1579, 1508, 1477, 1399, 1101, 985, 836, 768, 587, 567, 422, 413 cm^{-1}. ^1H NMR (400 MHz, $CDCl_3/Si(CH_3)_4$) δ = 8.51 (dd, J = 6.4, 0.8 Hz, 1H), 8.40 (d, J = 5.6 Hz, 1H), 8.22 (d, J = 8.0 Hz, 1H), 7.80−7.68 (m, 3H), 7.43 (d, J = 7.6 Hz, 1H), 7.14 (td, J = 6.8, 1.2 Hz, 1H), 7.10 (td, J = 5.2, 1.2 Hz, 1H), 6.66 (dd, J = 8.0, 1.2 Hz, 1H), 6.28 (td, J = 10.8, 2.4 Hz, 1H), 6.00 (s, 1H), 5.71 (dd, J = 9.0, 2.4 Hz, 1H), 5.22 (s, 1H), 2.06 (s, 3H), 1.81 (s, 3H), 1.79 (s, 3H). ESI-MS (m/z). Calcd for $C_{28}H_{23}N_2O_2F_2{}^{191}Ir$ (M^+): 648.1328. Found: 648.1327.

[{Ir(mpiq)$_2$(μ-Br)}$_2$] ***(19b)***.[17] **19b** was obtained as a red powder (25 mg, 98% yield) from ***fac*-10** (30 mg, 35 μmol) and $ZnBr_2$ (0.38 g, 1.7 mmol) using a precedure similar to that for **6b** (2.0 mL of 1,2-dichloroethane was used as the solvent). mp >300 °C. IR (ATR): ν = 1585, 1501, 1444, 1378, 1348, 1271, 1148, 1124, 1045, 867, 812, 782, 738, 671, 579, 483, 414 cm^{-1}. ^1H NMR (300 MHz, $CDCl_3/Si(CH_3)_4$) δ = 9.22 (d, J = 6.3 Hz, 4H), 8.93 (d, J = 8.4 Hz, 4H), 8.00−7.93 (m, 8H), 7.82 (t, J = 7.2 Hz, 4H), 7.76 (t, J = 7.2 Hz, 4H), 6.70 (d, J = 6.0 Hz, 4H), 6.62 (d, J = 6.6 Hz, 4H), 5.85 (s, 4H), 1.86 (s, 12H). ESI-MS (m/z). Calcd for $C_{64}H_{48}N_4Br_2Ir_2$ (M^+): 1416.1470. Found: 1416.1514.

DOI: 10.1021/acs.inorgchem.6b02270
Inorg. Chem. XXXX, XXX, XXX−XXX

fac-Ir(Cl-tpy)$_3$ (***fac*-20**).[17] A solution of ***fac*-2** (30 mg, 43 μmol) and $FeCl_3$ (58 mg, 2.2 mmol) in 1,2-dichloroethane (2.0 mL) was stirred at room temperature for 2 h. The solvent was removed by evaporation. The crude residue was purified by silica gel column chromatography using $CHCl_3$ as the eluent to give ***fac*-20** as a yellow powder (3.1 mg, 9% yield). mp >300 °C. IR (ATR): ν = 1598, 1467, 1421, 1255, 1063, 1043, 882, 779, 741, 614 cm^{-1}. ^{1}H NMR (300 MHz, $CDCl_3$/$Si(CH_3)_4$) δ = 7.79 (d, J = 7.8 Hz, 3H), 7.59 (t, J = 9.0 Hz, 3H), 7.58 (s, 3H), 7.42 (d, J = 5.7 Hz, 3H), 6.86 (t, J = 5.7 Hz, 3H), 6.63 (s, 3H), 2.16 (s, 9H). ESI-MS (m/z). Calcd for $C_{36}H_{27}N_3{}^{35}Cl_3{}^{191}Ir$ (M^+): 797.0871. Found: 797.0871.

[{Ir(F$_2$ppy)$_2$(μ-Br)}$_2$] (***23b*)**.[17] **23b** was obtained as a yellow powder (12 mg, 55% yield) from ***mer*-8** (25 mg, 33 μmol) and $ZnBr_2$ (0.46 mg, 2.0 mmol) using a precedure similar to that for **6b** (2.0 mL of 1,2-dichloroethane was used as the solvent). mp > 300 °C. IR (ATR): ν = 1599, 1572, 1557, 1478, 1402, 1293, 1248, 11660, 1102, 988, 829, 782, 753, 715, 708, 568, 527 cm^{-1}. ^{1}H NMR (300 MHz, $CDCl_3$/$Si(CH_3)_4$) δ = 9.40 (d, J = 5.1 Hz, 4H), 8.33 (d, J = 8.4 Hz, 4H), 7.87 (td, J = 8.1, 1.8 Hz, 4H), 6.91 (td, J = 6.9, 0.9 Hz, 4H), 6.33 (td, J = 11.1, 2.1 Hz, 4H), 5.28 (dd, J = 9.3, 2.1 Hz, 4H). ESI-MS (m/z). Calcd for $C_{44}H_{24}N_4F_8Br_2Ir_2$ (M^+): 1303.9460. Found: 1303.9467.

[{Ir(ppy)$_2$(μ-Br)}$_2$] (***24*)**.[17] **24** was obtained as a yellow powder (13 mg, 50% yield) from ***fac*-1** (30 mg, 46 μmol) and $ZnBr_2$ (0.51 g, 2.3 mmol) using a precedure similar to that for **6b** (2.0 mL of 1,2-dichloroethane was used as the solvent). mp >300 °C. IR (ATR): ν = 1605, 1580, 1477, 1421, 1157, 1030, 754, 740, 732, 724, 670, 629, 420 cm^{-1}. ^{1}H NMR (300 MHz, $CDCl_3$/$Si(CH_3)_4$) δ = 9.51 (d, J = 5.4 Hz, 4H), 7.89 (d, J = 7.8 Hz, 4H), 7.78 (td, J = 7.2, 1.2 Hz, 4H), 7.48 (d, J = 7.8 Hz, 4H), 6.86 (td, J = 6.6, 1.5 Hz, 4H), 6.74 (td, J = 6.9, 1.2 Hz, 4H), 6.58 (td, J = 5.1, 1.5 Hz, 4H), 5.92 (d, J = 7.8 Hz, 4H). ESI-MS (m/z). Calcd for $C_{44}H_{32}N_4Br_2Ir_2$ (M^+): 1160.0214. Found: 1160.0210.

[{Ir(mppy)$_2$(μ-Br)}$_2$] (***25*)**.[17] **25** was obtained as a yellow powder (20 mg, 80% yield) from ***fac*-3** (30 mg, 40 μmol) and $ZnBr_2$ (0.45 g, 2.0 mmol) using a precedure similar to that for **6b** (2.0 mL of 1,2-dichloroethane was used as the solvent). mp >300 °C. IR (ATR): ν = 1581, 1547, 1459, 1425, 1277, 1209, 1158, 1033, 769, 748, 586 cm^{-1}. ^{1}H NMR (300 MHz, $CDCl_3$/$Si(CH_3)_4$) δ = 9.44 (d, J = 6.3 Hz, 4H), 7.76−7.68 (m, 8H), 7.41 (d, J = 8.7 Hz, 4H), 6.77 (td, J = 6.3, 1.8 Hz, 4H), 6.35 (dd, J = 8.4, 2.4 Hz, 4H), 5.43 (d, J = 2.7 Hz, 4H), 3.41 (s, 12H). ESI-MS (m/z). Calcd for $C_{48}H_{40}N_4O_4Br_2Ir_2$ (M^+): 1280.0637. Found: 1280.0628.

[{Ir(Br-tpy)$_2$(μ-Br)}$_2$] (***26*)**.[17] **26** was obtained as a yellow powder (20 mg, 83% yield) from ***fac*-7** (30 mg, 32 μmol) and $ZnBr_2$ (0.36 g, 1.6 mmol) using a precedure similar to that for **6b** (2.0 mL of 1,2-dichloroethane was used as the solvent). mp >300 °C. IR (ATR): ν = 1606, 1574, 1558, 1471, 1422, 1358, 1267, 1221, 1156, 1068, 1039, 1016, 866, 776, 748, 604, 422 cm^{-1}. ^{1}H NMR (300 MHz, $CDCl_3$/$Si(CH_3)_4$) δ = 9.41 (d, J = 5.7 Hz, 4H), 7.82−7.77 (m, 8H), 7.62 (s, 4H), 6.89−6.85 (m, 4H), 5.69 (s, 4H), 1.98 (s, 12H). ESI-MS (m/z). Calcd for $C_{48}H_{36}N_4Br_6Ir_2$ (M^+): 1527.7238. Found: 1527.7202.

Ir(mppy)(F$_2$ppy)(acac) (***28*)** *and Ir(mppy)$_2$(acac)* (***29*)**.[17] **28** (yellow powder, 9.1 mg, 54% yield) and **29** (yellow powder, 2.0 mg, 13% yield) was obtained from ***mer*-14** (20 mg, 27 μmol), $ZnBr_2$ (0.30 g, 1.3 mmol), acetylacetone (6.0 mg, 54 μmol), and tetrabutylammonium hydroxide (TBAH) (25 mg, 40 μmol) using a procedure similar to that for **18**. The product was purified by silica gel column chromatography with hexanes/CH_2Cl_2 (4/1) as the eluent.

28. mp 261−263 °C. IR (ATR): ν = 2925, 1579, 1508, 1476, 1399, 1278, 1213, 1158, 1101, 1042, 984, 835, 768, 588, 567, 525, 420, 412 cm^{-1}. ^{1}H NMR (300 MHz, $CDCl_3$/$Si(CH_3)_4$) δ = 8.51 (dd, J = 5.4, 1.2 Hz, 1H), 8.36 (d, J = 5.7 Hz, 1H), 8.22 (d, J = 7.8 Hz, 1H), 7.75−7.69 (m, 3H), 7.50 (d, J = 8.7 Hz, 1H), 7.14 (td, J = 6.3, 1.2 Hz, 1H), 7.08 (td, J = 6.3, 2.1 Hz, 1H), 6.66 (dd, J = 8.0, 1.2 Hz, 1H), 6.28 (td, J = 10.8, 2.4 Hz, 1H), 5.72 (dd, J = 8.7, 2.7 Hz, 1H), 5.69 (d, J = 2.7 Hz, 1H), 5.20 (s, 1H), 3.55 (s, 3H), 1.80 (s, 3H), 1.79 (s, 3H). ESI-MS (m/z). Calcd for $C_{28}H_{23}N_2O_3F_2{}^{191}Ir$ (M^+): 664.1277. Found: 664.1282.

29. mp >300 °C. IR (ATR): ν = 2923, 1579, 1508, 1477, 1399, 1101, 985, 836, 768, 587, 567, 422, 413 cm^{-1}. ^{1}H NMR (300 MHz, $CDCl_3$/$Si(CH_3)_4$) δ = 8.43 (d, J = 5.4 Hz, 2H), 7.72−7.63 (m, 4H), 7.47 (d, J = 8.7 Hz, 2H), 7.04 (td, J = 6.3, 1.8 Hz, 2H), 6.40 (dd, J = 8.7, 2.4 Hz, 2H), 5.77 (d, J = 2.7 Hz, 2H), 5.20 (s, 1H), 3.53 (s, 6H), 1.78 (s, 6H). ESI-MS (m/z). Calcd for $C_{29}H_{27}N_2O_4{}^{191}Ir$ (M^+): 658.1571. Found: 658.1578.

Ir(mpiq)(F$_2$ppy)(acac) (***30*)**.[17] **30** was prepared as an orange powder (12 mg, 67% yield from ***mer*-15**) from ***mer*-15** (20 mg, 24 μmol), $ZnBr_2$ (0.27 g, 1.2 mmol), acetylacetone (6.0 mg, 54 μmol), and tetrabutylammonium hydroxide (TBAH) (25 mg, 40 μmol) using a precedure similar to that for **18**. The product was purified by silica gel column chromatography with hexanes/CH_2Cl_2 (2/1) as the eluent. mp >300 °C. IR (ATR): ν = 1566, 1557, 1515, 1391, 1290, 1265, 1245, 1100, 985, 835, 813, 782, 753, 737, 714, 672, 588, 574, 567, 526 cm^{-1}. ^{1}H NMR (300 MHz, $CDCl_3$/$Si(CH_3)_4$) δ = 8.98−8.94 (m, 1H), 8.52 (d, J = 5.4 Hz, 1H), 8.33 (d, J = 6.3 Hz, 1H) 8.27 (d, J = 8.4 Hz, 1H), 8.10 (d, J = 8.1 Hz, 1H), 7.93−7.90 (m, 1H), 7.77 (t, J = 7.5 Hz, 1H), 7.72−7.69 (m, 2H), 7.44 (d, J = 6.0 Hz, 1H), 7.18 (td, J = 6.6, 1.2 Hz, 1H), 6.76 (dd, J = 7.8, 2.1 Hz, 1H), 6.28 (td, J = 10.2, 2.1 Hz, 1H), 6.15 (s, 1H), 5.70 (dd, J = 8.7, 2.4 Hz, 1H), 5.21 (s, 1H), 2.12 (s, 3H), 1.82 (s, 3H), 1.73 (s, 3H). ESI-MS (m/z). Calcd for $C_{32}H_{25}N_2O_2F_2{}^{191}Ir$ (M^+): 698.1484. Found: 698.1476.

Ir(mpiq)$_2$(acac) (***31*)**.[17] **31** was prepared for the characterization of the products of degradation reaction of ***mer*-15** (to prove that only **30** was produced, not **31**, from ***mer*-15**). A solution of **19b** (10 mg, 7.0 μmol), tetrabutylammonium hydroxide (TBAH) (13 mg, 21 μmol) and acetylacetone (5 mg, 50 μmol) in CH_2Cl_2/MeOH (10/1, 1.1 mL) was refluxed for 14 h. After cooling to room temperature, water was added to the reaction mixture and extracted with $CHCl_3$. The combined organic layer was dried over Na_2SO_4. After filtration, the filtrate was evaporated under reduced pressure and the resulting residue was purified by silica gel chromatography using hexanes/CH_2Cl_2 (5/1) as the eluent to give **31** as a red powder (8.9 mg, 89% yield). mp >300 °C. IR (ATR): ν = 3021, 1576, 1513, 1502, 1437, 1395, 1373, 1350, 1271, 1252, 1148, 1123, 1049, 1014, 869, 813, 741, 733, 671, 584, 576, 415, 396 cm^{-1}. ^{1}H NMR (300 MHz, $CDCl_3$/$Si(CH_3)_4$) δ = 9.00−8.97 (m, 2H), 8.41 (d, J = 6.3 Hz, 2H), 8.10 (d, J = 8.4 Hz, 2H), 7.93−7.90 (m, 2H), 7.73−7.68 (m, 4H), 7.42 (d, J = 6.6 Hz, 2H), 6.71 (dd, J = 9.0, 1.8 Hz, 2H), 6.23 (s, 2H), 5.16 (s, 1H), 2.02 (s, 6H), 1.73 (s, 6H). ESI-MS (m/z). Calcd for $C_{37}H_{31}N_2O_2{}^{191}Ir$ (M^+): 726.1986. Found: 726.1979.

Ir(tpy)(F$_2$ppy)(8BSQ$^-$) (***35a*)**.[17] A solution of ***mer*-12** (10 mg, 14 μmol) and $ZnBr_2$ (0.20 g, 0.89 mmol) in 1,2-dichloroethane (1.0 mL) was refluxed for 4 h. After the precipitate was filtered off and the filtrate was concentrated under reduced pressure, the resulting residue was purified by silica gel column chromatography using $CHCl_3$ as the eluent to give the mixture of **6b** and **27b** as a yellow powder (6.4 mg, 72% yield assuming that only **27b** was obtained).

The next step was carried out according to our previous report.[19] The obtained mixture of **6b** and **27b** (6.4 mg, 5.2 μmol) was dissolved in a mixture of CH_2Cl_2/EtOH (4/1, 1.3 mL), and 8-benzenesulfonylamidoquinoline (5.0 mg, 18 μmol) and triethylamine (38 mg, 0.37 mmol) were then added. The reaction mixture was refluxed at 80 °C for 1 h. The solvent was evaporated under reduced pressure and the residue purified by silica gel chromatography with $CHCl_3$ as the eluent to give the stereoisomer mixture of **35** as a brown powder (4.1 mg, 36% yield from ***mer*-12**). The stereoisomer mixture of **35** was subjected to further purification by silica gel column chromatography eluted with hexanes/$CHCl_3$/THF (4/1/1) to afford **35a** as a brown powder (1.0 mg, 10% yield from ***mer*-12**). mp >300 °C. IR (ATR): ν = 2923, 1579, 1508, 1477, 1399, 1101, 985, 836, 768, 587, 567, 422, 413 cm^{-1}. ^{1}H NMR (300 MHz, $CDCl_3$/$Si(CH_3)_4$) δ = 9.20 (dd, J = 5.7, 0.6 Hz, 1H), 8.22−8.16 (m, 2H), 8.06 (dd, J = 8.7 1.5 Hz, 1H) 7.75−7.64 (m, 3H), 7.54−7.52 (m, 1H), 7.46 (t, J = 8.1 Hz, 1H), 7.36 (d, J = 8.1 Hz, 1H), 7.25−7.12 (m, 6H), 7.04−6.96 (m, 3H), 6.71−6.68 (m, 2H), 6.41 (td, J = 10.8, 2.4 Hz, 1H), 6.05 (s, 1H), 5.64 (dd, J = 8.7, 2.1 Hz, 1H), 2.12 (s, 3H). ESI-MS (m/z). Calcd for $C_{38}H_{27}N_4O_2F_2S{}^{191}Ir$ (M^+): 832.1423. Found: 832.1426.

Ir(tpy)$_2$(8BSQ$^-$) (***36*)**.[17] The authentic sample of **36** was prepared as described in our previous report to characterize the products of the degradation reactions of ***mer*-12** (Table 7).[19] A solution of the chloro-bridged Ir dimer [{Ir(tpy)$_2$(μ-Cl)}$_2$] **6a** (52 mg, 45 μmol), 8-

DOI: 10.1021/acs.inorgchem.6b02270
Inorg. Chem. XXXX, XXX, XXX−XXX

benzenesulfonylamidoquinoline (28 mg, 97 μmol), and triethylamine (0.20 mg, 2.0 mmol) in CH_2Cl_2/EtOH (4/1, 2.5 mL) was stirred at room temperature for 10 min. The solvent was evaporated under reduced pressure and the residue was purified by silica gel chromatography with $CHCl_3$ as the eluent to give **36** as a brown powder (68 mg, 95% yield), mp >300 °C. IR (ATR): ν = 1588, 1562, 1475, 1459, 1381, 1311, 1138, 1109, 1086, 942, 849, 822, 746, 689, 580, 566, 528, 427 cm^{-1}. ^1H NMR (300 MHz, $CDCl_3/Si(CH_3)_4$) δ = 9.12 (dd, J = 4.8, J = 0.9 Hz, 1H), 8.15 (dd, J = 7.8, 1.2 Hz, 1H), 8.00 (dd, J = 8.4, 1.2 Hz, 1H), 7.73−7.66 (m, 3H), 7.61−7.52 (m, 2H), 7.46−7.36 (m, 3H), 7.29 (d, J = 6.6 Hz, 1H), 7.19−7.09 (m, 5H), 7.00−6.91 (m, 3H), 6.74−6.64 (m, 3H), 6.13 (s, 1H), 5.97 (s, 1H), 2.10 (s, 3H), 2.08 (s, 3H). ESI-MS (m/z). Calcd for $C_{39}H_{31}N_4O_2S^{191}Ir$ (M^+): 810.1768. Found: 810.1759. Anal. Calcd for $C_{39}H_{31}N_4O_2SIr\cdot 0.1CHCl_3$: C, 57.00; H, 3.80; N, 6.80. Found: C, 56.73; H, 3.78; N, 6.56.

*mer-Ir(tpy) (Br-tpy)(F$_2$ppy) (**mer-43**).*[17] A solution of ***mer*-12** (11 mg, 15 μmol) and NBS (3.0 mg, 17 μmol) in CH_2Cl_2 (2 mL) was stirred at room temperature for 1 h. The solvent was removed under reduced pressure and the resulting residue was purified by silica gel chromatography using hexanes/$CHCl_3$ (4/1) as the eluent to give ***mer*-43** as a yellow powder (7.1 mg, 64% yield), mp >300 °C. IR (ATR): ν = 1581, 1552, 1469, 1420, 1391, 1261, 1233, 1157, 1096, 980, 874, 771, 748, 603, 568, 522, 428 cm^{-1}. ^1H NMR (300 MHz, $CDCl_3/Si(CH_3)_4$) δ = 8.30 (d, J = 11 Hz, 1H), 7.98 (dd, J = 5.7, 0.9 Hz, 1H), 7.93 (dd, J = 5.7, 0.9 Hz, 1H), 7.75 (t, J = 5.7 Hz, 3H), 7.66−7.49 (m, 5H), 6.88 (td, J = 6.6, 1.2 Hz, 1H), 6.81−6.71 (m, 3H), 6.42−6.34 (m, 2H), 6.30 (s, 1H), 6.23 (s, 1H), 2.16 (s, 3H), 2.14 (s, 3H). ESI-MS (m/z). Calcd for $C_{35}H_{25}N_3F_2{}^{79}Br^{191}Ir$ (M^+): 795.0800. Found: 795.0800.

X-ray Data Collection and Refinement. All crystalline samples of the Ir complexes were recrystallized from hexanes/CH_2Cl_2 (for ***fac*-12**, ***mer*-12**, ***mer*-15**, **6b**, and **35a**) or hexanes/$CHCl_3$ (for ***mer*-43**) to give crystals suitable for single-crystal X-ray analysis. Single-crystal X-ray studies were performed on a Bruker APEX CCD diffractometer equipped with a Bruker Instruments low-temperature attachment. Data were collected at 103 K (for **35a**), 173 K (for ***fac*-12**, ***mer*-12**, ***mer*-15**, and ***mer*-43**), or 296 K (for **6b**) using graphite-monochromated Mo−K α radiation (λ = 0.71073 Å). The frames were indexed, integrated, and scaled using the SMART and SAINT software packages.[20] An empirical absorption correction was applied to the collected reflections with SADABS[21] using XPREP.[22] All of the structures were solved by the direct method using the program SHELXS-97 and were refined on F^2 by the full-matrix leastsquares technique using the SHELXL-97 program package.[23] All non-hydrogen atoms were refined anisotropically in the structure. All crystal data in this manuscript can be obtained free of charge from The Cambridge Crystallographic Data Centre via www.ccdc.cam.ac.uk/data_request/cif.

*Crystal Data for **6b**.* $C_{48}H_{40}Br_2Ir_2N_4$, Mr = 1217.06, monoclinic, $P2_1/n$, a = 11.6206(6), b = 14.8110(7), c = 25.0132(13) Å, β = 96.241(2), V = 4279.6(4) Å^3, Z = 4, ρ_{calc} = 1.889 g·cm^{-3}, R = 0.0650 (for 5375 reflection with $I > 2\sigma(I)$), Rw = 0.1570 (for 7525 reflections), GOF = 1.139. CCDC 1501488 contains the supplementary crystallographic data for the paper.

*Crystal Data for **fac-12**.* $C_{35}H_{26}F_2IrN_3$, Mr = 718.79, monoclinic, $C2/c$, a = 34.105(16), b = 9.227(4), c = 17.928(8) Å, β = 99.7100(2), V = 5561(5) Å^3, Z = 8, ρ_{calc} = 1.717 g.cm^{-3}, R = 0.0484 (for 5437 reflections with $I > 2\sigma(I)$), Rw = 0.1094 (for 6249 reflections), GOF = 1.137. CCDC 1501443 contains the supplementary crystallographic data for the paper.

*Crystal Data for **mer-12**.* $C_{35}H_{26}F_2IrN_3\cdot CH_2Cl_2$, Mr = 803.71, monoclinic, $P2/c$, a = 19.6105(16), b = 8.6627(7), c = 17.9826(15) Å, β = 96.5980(1), V = 3024.6(4) Å^3, Z = 4, ρ_{calc} = 1.759 g·cm^{-3}, R = 0.0366 (for 5970 reflection with $I > 2\sigma(I)$), Rw = 0.0972 (for 6870 reflections), GOF = 1.042. CCDC 1502134 contains the supplementary crystallographic data for the paper.

*Crystal Data for **mer-15**.* $C_{43}H_{30}F_2IrN_3\cdot CH_2Cl_2$, Mr = 903.83, triclinic, $P\bar{1}$, a = 10.878(3), b = 12.483(4), c = 13.740(4) Å, α = 76.509(5), β = 73.212(5), γ = 89.340(6)°, V = 1733.9(9) Å^3, Z = 2, ρ_{calc} = 1.731 g·cm^{-3}, R = 0.0582 (for 5600 reflection with $I > 2\sigma(I)$), Rw = 0.1103 (for 6426 reflections), GOF = 1.140. CCDC 1501444 contains the supplementary crystallographic data for the paper.

*Crystal Data for **35a**.* $C_{38}H_{27}F_2IrN_4O_2S$, Mr = 833.90, triclinic, $P\bar{1}$, a = 10.215(5), b = 10.959(5), c = 16.413(5) Å, α = 80.353(5), β = 86.921(5), γ = 71.791(5)°, V = 1720.7(13) Å^3, Z = 2, ρ_{calc} = 1.610 g.cm^{-3}, R = 0.0623 (for 5131 reflection with $I > 2\sigma(I)$), Rw = 0.1380 (for 6240 reflections), GOF = 1.050. CCDC 1501455 contains the supplementary crystallographic data for the paper.

*Crystal Data for **mer-43**.* $C_{35}H_{25}BrF_2IrN_3\cdot 1.5H_2O$, Mr = 821.69, triclinic, $P\bar{1}$, a = 9.5171(7), b = 12.9204(9), c = 13.0846(10) Å, α = 70.745(1), β = 86.152(1), γ = 84.710(1)°, V = 1511.32(19) Å^3, Z = 2, ρ_{calc} = 1.806 g·cm^{-3}, R = 0.0311 (for 5767 reflection with $I > 2\sigma(I)$), Rw = 0.0893 (for 5992 reflections), GOF = 1.066. CCDC 1504245 contains the supplementary crystallographic data for the paper.

Measurements of UV/vis Absorption and Luminescence Spectra. UV/vis spectra were recorded on a JASCO V-550 UV/vis spectrophotometer and emission spectra were recorded at 298 K on JASCO FP-6200 and FP-6500 spectrofluorometers, respectively. Sample solutions in quartz cuvettes equipped with Teflon septum screw caps were degassed by bubbling Ar through the solution for 10 min prior to conducting the luminescence measurements. Phosphorescence quantum yields (Φ) were determined using quinine sulfate (Φ = 0.55 in 0.1 M H_2SO_4)[24] or *fac*-Ir(mpiq)$_3$ (***fac*-10**) (Φ = 0.26 in toluene).[25] Equation 1 was used to calculate the emission quantum yields, in which Φ_s and Φ_r denote the quantum yields of the sample and the reference compound, respectively. The η_s and η_r terms are the refractive indexes of the solvents used for the measurements of the sample and the reference (η: 1.477 for DMSO, 1.333 for H_2O, and 1.497 for toluene). The A_s and A_r terms are the absorbance of the sample and the reference, and the I_s and I_r terms stand for the integrated areas under the emission spectra of the sample and reference, respectively (all of the Ir compounds were excited at 366 nm for luminescence measurements in this study).

$$\Phi_s = \Phi_r(\eta_s^2 A_r I_s)/(\eta_r^2 A_s I_r) \quad (1)$$

The luminescence lifetimes of sample solutions of Ir(III) complexes in degassed DMSO at 298 K were measured on a TSP1000-M-PL (Unisoku, Osaka, Japan) instrument by using THG (355 nm) of Nd:YAG laser, Minilite I (Continuum, CA, USA) as excitation source. The signals were monitored with an R2949 photomultiplier. Data were analyzed using a single exponential decay equation (for ***mer*-12−16**, ***fac*-12**, **17**, **18**, **22b**, and **28-31**) or a biexponential decay equation (for **33**, **35a**, and **36**). Sample solutions in quartz cuvettes equipped with Teflon septum screw caps were degassed by bubbling Ar through the solution for 20 min prior to measuring the lifetime.

RESULTS AND DISCUSSION

Synthesis of Cyclometalated Ir Complexes. The substrates for the decomposition reactions, bis- or tris-cyclometalated Ir complexes, were synthesized from $IrCl_3\cdot 3H_2O$ and cyclometalating ligands. The facial (*fac*) isomers of the cyclometalated homoleptic Ir complexes, Ir(ppy)$_3$ (***fac*-1**), Ir(tpy)$_3$ (***fac*-2**), and Ir(F$_2$ppy)$_3$ (***fac*-8**) were synthesized at 200 °C and their meridional (*mer*) isomers were obtained at ca. 150 °C, as reported by Thompson and co-workers.[1h] For example, the synthesis of ***fac*-2**, ***mer*-2**, ***fac*-10**, ***mer*-10**, ***fac*-12**, ***mer*-12** and ***mer*-15** is shown in Chart 6. Although negligible amounts of *fac*-Ir(tpy)$_2$(F$_2$ppy) (***fac*-12**) were obtained by Thompson's method (a mixture of chloro-bridged Ir dimer [{Ir(tpy)$_2$(μ-Cl)}$_2$] **6a**, which was prepared from $IrCl_3\cdot 3H_2O$ and tpy,[26] and F$_2$ppy in glycerol was refluxed at 200 °C) due to ligand sclambling,[27] it was successfully obtained from the same substrates by using AgOTf in 2-ethoxyethanol.[28] Meridional isomers of heteroleptic Ir complexes, ***mer*-12**, ***mer*-14**, and ***mer*-15**, were obtained in 74%, 17%, and 81% yields, respectively, from the corresponding μ-complexes and ligands and ***mer*-13**

DOI: 10.1021/acs.inorgchem.6b02270
Inorg. Chem. XXXX, XXX, XXX−XXX

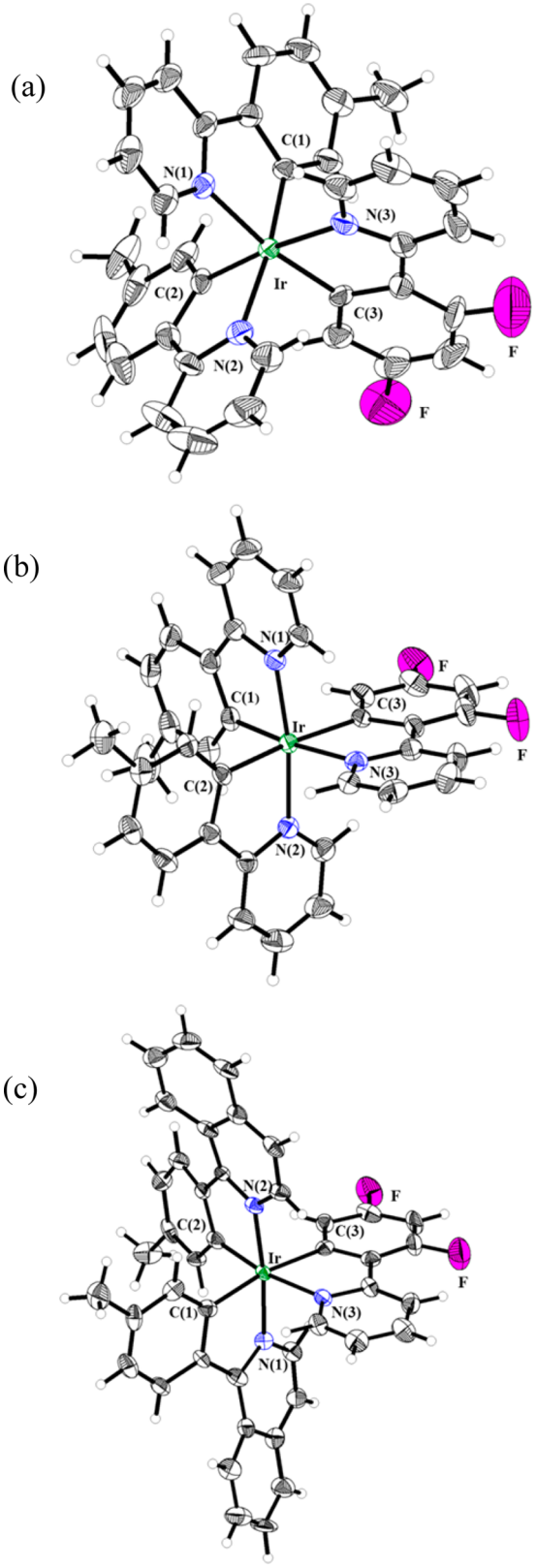

Figure 1. ORTEP drawings of single crystal structures of (a) ***fac*-12**, (b) ***mer*-12**, and (c) ***mer*-15** with 50% probability ellipsoids. For clarity, the CH_2Cl_2 in b and c is omitted.

and ***mer*-16** were synthesized according to a method reported in a patent,[29] in which the μ-complex $[Ir(F_2ppy)_2(\mu\text{-}Cl)]_2$ was reacted with tpy (for ***mer*-13**) or mpiq (for ***mer*-16**) in the presence of AgOTf and NEt_3. The synthesis of ***fac*-** and ***mer*-10** was carried out as shown in Chart 6.

Table 1. Selected Bond Lengths (Å) of (a) *fac*-12, (b) *mer*-12, and (c) *mer*-15 in X-ray Crystal Structure (left) and Those Obtained by DFT Calculations (right)

(a)	X-ray structure bond lengths (Å)	calculated bond lengths (Å)
Ir−C(l) (tpy)	2.01	2.04
Ir−C(2) (tpy)	1.99	2.04
Ir−C(3) (F_2ppy)	1.99	2.03
Ir−N(l) (tpy)	2.12	2.17
Ir−N(2) (tpy)	2.12	2.16
Ir−N(3) (F_2ppy)	2.13	2.16
(b)	X-ray structure bond lengths (Å)	calculated bond lengths (Å)
Ir−C(l) (tpy)	1.99	2.02
Ir−C(2) (tpy)	2.04	2.09
Ir−C(3) (F_2ppy)	2.07	2.11
Ir−N(l) (tpy)	2.02	2.07
Ir−N(2) (tpy)	2.03	2.08
Ir−N(3) (F_2ppy)	2.11	2.19
(c)	X-ray structure bond lengths (Å)	calculated bond lengths (Å)
Ir−C(l) (mpiq)	1.97	2.02
Ir−C(2) (mpiq)	2.05	2.08
Ir−C(3) (F_2ppy)	2.08	2.10
Ir−N(l) (mpiq)	2.02	2.09
Ir−N(2) (mpiq)	2.03	2.08
Ir−N(3) (F_2ppy)	2.12	2.20

All the Ir complexes were structurally characterized by ^{1}H NMR, ESI-MS and related techniques, and X-ray structure analyses were carried out for ***fac*-12**, ***mer*-12**, and ***mer*-15** (ORTEP drawings[30] in Figure 1). As summarized in Table 1, selected bond lengths of ***fac*-12** are quite similar to those of *fac*-Ir(tpy)$_3$ (***fac*-2**) (Ir−C 2.02 Å and Ir−N 2.13 Å).[1h] It should be noted that the Ir−C and Ir−N bond lengths of F_2ppy ligand in ***mer*-12** (Ir−C 2.07 Å and Ir−N 2.11 Å) and ***mer*-15** (Ir−C 2.08 Å and Ir−N 2.12 Å) are somewhat longer than those between Ir and tpy ligands (Ir−C 1.99, 2.04 Å and Ir−N 2.02, 2.03 Å) and Ir and mpiq ligands (Ir−C 1.97, 2.05 Å and Ir−N 2.02, 2.03 Å). For these Ir complexes, the Ir−C and Ir−N bond lengths were estimated by DFT calculations and are listed in Table 1, because these calculated values are important in terms of the mechanism of the degradation reactions, as described below (the results of DFT calculations of other tris-cyclometalated homoleptic Ir complexes, ***fac*-2**, ***fac*-3**, ***fac*-7**, ***fac*-8**, and ***fac*-9**, are shown in Figure S23 in the Supporting Information). The experimental Ir−C and Ir−N bond lengths of ***fac*-12**, ***mer*-12**, and ***mer*-15** are in good agreement with the calculated Ir−C and Ir−N bond lengths (DFT calculations in Table 1).

Degradation Reaction of *fac*-Ir(tpy)$_3$ by Brønsted or Lewis Acids. The results for the Brønsted or Lewis acid-promoted degradation reactions of *fac*-Ir(tpy)$_3$ (***fac*-2**) in 1,2-dichloroethane are summarized in Table 2. The reaction of ***fac*-2** with $AlCl_3$ gave the corresponding chloro-bridged Ir dimer, **6a**, in 84% yield (Entry 1). It was found that $ZnCl_2$ and $ZnBr_2$ promoted the degradation of ***fac*-2** at reflux temperature to provide **6a** and the bromo-bridged Ir dimer **6b**, respectively, in reasonably good yields, while that reaction negligibly proceeds at room temperature (Entries 2−4). In Entry 3, the tpy ligand was recovered in ca. 30% yield, as determined by ^{1}H NMR

DOI: 10.1021/acs.inorgchem.6b02270
Inorg. Chem. XXXX, XXX, XXX−XXX

Table 2

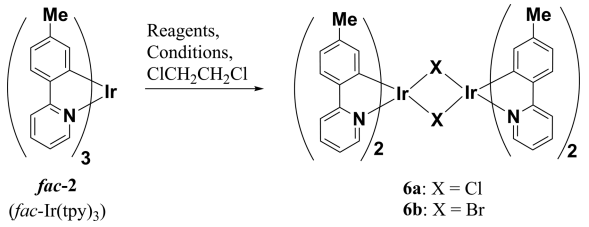

***fac*-2** (*fac*-Ir(tpy)$_3$)

6a: X = Cl
6b: X = Br

entry	reagents	reaction conditions	recovery yield of ***fac*-2** (*fac*-Ir(tpy)$_3$) (%)	yield of **6** (%)
1	$AlCl_3$ (5.0 equiv)	r.t., 30 min	trace	84 (**6a**)
2	$ZnCl_2$ (50 equiv)	r.t., 1.5 h	88	trace
3	$ZnCl_2$ (80 equiv)	reflux, 2 h	trace	52 (**6a**)
4	$ZnBr_2$ (50 equiv)	reflux, 3 h	trace	93 (**6b**)
5	ZnO (50 equiv)	reflux, 48 h	66	trace
6	ZnO (25 equiv), $(n\text{Bu})_4\text{NBr}$ (50 equiv)	reflux, 96 h	90	trace
7	$Zn(ClO_4)_2\cdot 6H_2O$ (10 equiv)[a]	r.t., 48 h	85	trace
8	$ZnCl_2$ (50 equiv)[a]	reflux, 13 h	15	trace
9	$ZnCl_2$ (50 equiv)[b]	reflux, 10 h	trace	14
10	Me_3SiCl (50 equiv)	r.t., 2.5 h	trace	71 (**6a**)
11	$FeCl_3$ (50 equiv)	r.t., 2 h	trace	trace[c]
12	$CuCl_2$ (5 equiv)	reflux, 44 h	trace	trace[d]
13	$PdCl_2$ (5 equiv)	reflux, 28 h	trace	trace
14	$CdCl_2\cdot 2.5H_2O$ (5 equiv)	reflux, 48 h	58	trace
15	Zn^{2+}-cyclen(H_2O) (**21a**) (10 equiv)	reflux, 12 h	100	trace
16	Cyclen·$ZnCl_2$ (**21b**) (10 equiv)	reflux, 16 h	23	trace
17	TFA (60 equiv), $(n\text{Bu})_4\text{NCl}$ (10 equiv)	r.t. 20 min	trace	<42[e] (**6a**)
18	TFA (60 equiv), $ZnCl_2$ (60 equiv)	r.t. 10 min	trace	trace
19	HCl (4 M in 1,4-dioxane) (50 equiv)	r.t., 1 h	trace	68 (**6a**)
20	$BF_3\cdot Et_2O$ (5 equiv), $(n\text{Bu})_4\text{NCl}$ (10 equiv)	r.t., 6 h	trace	trace[f]

[a]EtOH was used as the solvent. [b]CCl_4 was used as the solvent. [c]***fac*-20** was obtained in 9%. [d]See ref 32. [e]A mixture contaning **6a** was obtained. [f]See ref 35.

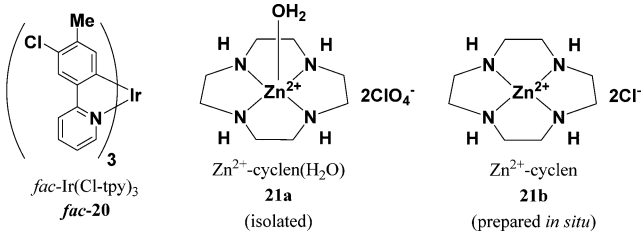

fac-Ir(Cl-tpy)$_3$
***fac*-20**

Zn^{2+}-cyclen(H_2O)
21a
(isolated)

Zn^{2+}-cyclen
21b
(prepared *in situ*)

(when 20−30 equiv of $ZnCl_2$ was used, tpy was recovered in 71−90%). Characterization of **6b** obtained in Entry 4 was carried out by ^{1}H NMR, ESI-MS, and X-ray structure analysis (See Figure 2). The representative parameters for the crystal structure of **6b** in Table 3 indicate that two Ir atoms of **6b**

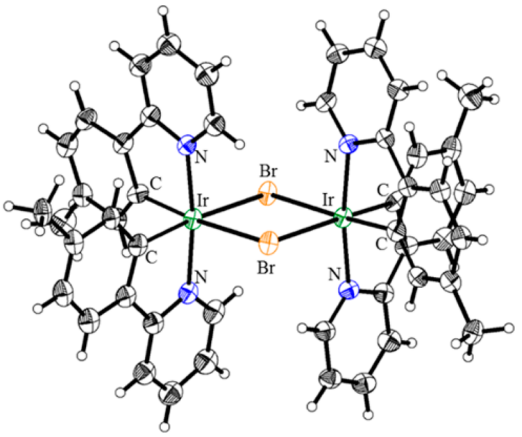

Figure 2. ORTEP drawing of single crystal structure of **6b** with 50% probability ellipsoids.

Table 3. Selected Bond Lengths (Å) and Selected Bond Angles (deg) of 6b

(a)	bond length (Å)
Ir−C (tpy)	2.01, 2.01, 2.02, 2.02
Ir−N (tpy)	2.04, 2.04, 2.05, 2.06
Ir−Br	2.62, 2.62, 2.65, 2.65
(b)	bond angles (deg)
N (tpy)−Ir−Br	91.2, 91.3, 93.4, 93.7
Br−Ir−Br	84.1, 84.3
Ir−Br−Ir	95.7, 95.8

Chart 7

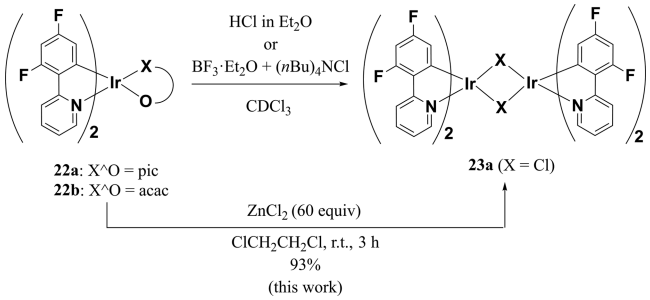

adopt a slightly distorted octahedral coordination geometry about the Ir(III) centers, at which two Ir−N bonds connected to the same Ir atom are in a *trans* configuration and the Ir−C bonds have cis configuration.[31] The degradation reaction of ***fac*-2** was not promoted by ZnO in the absence or the presence of $(n\text{Bu})_4\text{NBr}$ as a bromide source (Entries 5 and 6). In Entries 7−9, the reaction of ***fac*-2** with $Zn(ClO_4)_2$ or $ZnCl_2$ in EtOH and CCl_4 gave **6a** in negligible or very low yields. Trimethylsilyl chloride (TMSCl) also promoted the degradation of ***fac*-2** to give **6a** in 71% (Entry 10) and $FeCl_3$ gave the chlorinated ***fac*-2** (*fac*-Ir(Cl-tpy) (***fac*-20**)) and the chlorinated tpy ligand in 9% and 4% yields and other organic compounds could not be isolated (Entry 11), suggesting a possibility that ***fac*-2** was decomposed after chlorination, while $CuCl_2$ and $PdCl_2$ afforded complex mixtures, the characterization of which was difficult (Entries 12 and 13).[32] A negligible amount of **6a** was obtained after the reaction of $CdCl_2\cdot 2.5H_2O$ and Zn^{2+}−1,4,7,10-tetraazacyclodecane (Zn^{2+}-cyclen) complex (**21a**, **b**)[33,34] and afforded byproducts, characterization of which were difficult (Entries 14−16). The reaction with TFA and $(n\text{Bu})_4\text{NCl}$

DOI: 10.1021/acs.inorgchem.6b02270
Inorg. Chem. XXXX, XXX, XXX−XXX

Table 4

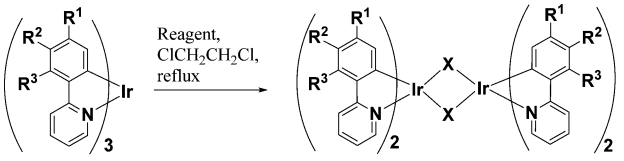

6b: R^1 = Me, R^2 = R^3 = H, X = Br
23b: R^1 = R^3 = F, R^2 = H, X = Br
24: R^1 = R^2 = R^3 = H, X = Br
25: R^1 = OMe, R^2 = R^3 = H, X = Br
26: R^1 = Me, R^2 = Br, R^3 = H, X = Br

entry	tris-cyclometalated Ir complex	R^1	R^2	R^3	reagents	reaction time (h)	yield of halogen-bridged Ir dimer (%)	recovery of S.M. (%)
1	*fac*-**1**	H	H	H	$ZnBr_2$ (50 equiv)	4.5	50 (**24**)	trace
2	*mer*-**1**	H	H	H	$ZnBr_2$ (50 equiv)	1	47 (**24**)	trace
3	*fac*-**2**	Me	H	H	$ZnBr_2$ (50 equiv)	3	93 (**6b**)	trace
4	*mer*-**2**	Me	H	H	$ZnBr_2$ (50 equiv)	2	33 (**6b**)	trace
5	*fac*-**3**	OMe	H	H	$ZnBr_2$ (50 equiv)	5	70 (**25**)	13
6	*fac*-**3**	OMe	H	H	$ZnBr_2$ (50 equiv)	20	80 (**25**)	trace
7	*fac*-**7**	Me	Br	H	$ZnBr_2$ (50 equiv)	5	25 (**26**)	60
8	*fac*-**7**	Me	Br	H	$ZnBr_2$ (50 equiv)	25	83 (**26**)	trace
9	*fac*-**8**	F	H	F	$ZnBr_2$ (60 equiv)	24	trace	74
10	*fac*-**8**	F	H	F	HCl (60 equiv)[a]	19	trace	78
11	*mer*-**8**	F	H	F	$ZnBr_2$ (60 equiv)	25	55 (**23b**)	23
12	*fac*-**9**	Me	NO_2	H	$ZnBr_2$ (60 equiv)	28	trace	100
13	*fac*-**9**	Me	NO_2	H	HCl (60 equiv)[a]	19	trace	95

[a]4 M HC1 in 1,4-dioxane was used.

Table 5

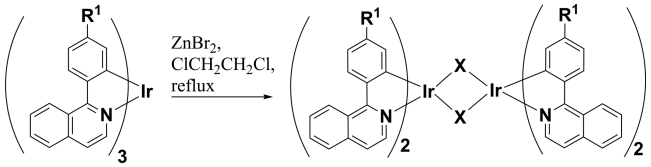

19b: R^1 = Me, X = Br
19c: R^1 = CF_3, X = Br

entry	tris-cyclometalated Ir complex	R^1	$ZnBr_2$ (equiv)	reaction time (h)	yield of halogen-bridged Ir dimer **19** (%)	recovery of S.M. (%)
1	*fac*-**10**	Me	60	3	98 (**19b**)	trace
2	*mer*-**10**	Me	60	1	67 (**19b**)	trace
3	*fac*-**11**	CF_3	60	24	<49[a] (**19c**)	51

[a]A mixture contaning **19c** was obtained.

afforded **6a** in less than 42% yield, as determined by ^{1}H NMR (Entry 17). On the other hand, the treatment with TFA and $ZnCl_2$ resulted in negligible amounts of **6a** (Entry 18).

Baranoff and co-workers reported that HCl (2 M in Et_2O) and $BF_3{\cdot}Et_2O$ promote the degradation of heteroleptic Ir complexes that contain an ancillary ligand, such as Ir-$(F_2ppy)_2$(pic) (pic picolinate) **22a** or Ir$(F_2ppy)_2$(acac) **22b** to give the corresponding Ir dimer $[Ir(F_2ppy)_2(\mu\text{-Cl})]_2$ **23a** (Chart 7).[9d] For comparison, the degradation of *fac*-**2** by hydrochloric acid (4 M HCl in 1,4-dioxane) gave **6a** in 68% yield (Entry 19 of Table 2), while the treatment of *fac*-**2** with 2 M HCl aq. in THF/H_2O (2/1) was negligible, suggesting that H_3O^+ (pK_a = −1.74) generated by leveling effect is not a sufficiently strong acid to decompose *fac*-**2**. Only trace amount of **6a** was obtained in the case of $BF_3{\cdot}Et_2O$ and $(n\text{Bu})_4$NCl (added as a Cl^- source) (Entry 20).[35] In this work, it was found that **22b** undergoes decomposition in the presence of $ZnCl_2$ (60 equiv) in 1,2-dichroloethane at room temperature to give **23a** in 93% yield (Chart 7). These results indicate that $AlCl_3$, $ZnCl_2$, $ZnBr_2$, TMSCl, and HCl/1,4-dioxane promote the degradation of *fac*-**2** to give **6a** or **6b** in moderate good yields and that the reactivity of tris-cyclometalated Ir complexes such as *fac*-**2** is different from bis-cyclometalated Ir complexes such as **22**.

Degradation Reaction of Tris-Cyclometalated Homoleptic Ir Complexes by $ZnBr_2$. The reactivity of other tris-cyclometalated Ir complexes with $ZnBr_2$ or HCl (4 M in 1,4-dioxane) was examined and the results are summarized in Tables 4 and 5. The decomposition of *fac*-**1**, *mer*-**1**, *fac*-**2**, *mer*-**2**, and *fac*-**3** by $ZnBr_2$ provided the corresponding bromo-bridged Ir dimers **24**, **6b**, and **25** as major products (Entries 1−6 in Table 4). The μ-complex **26** was obtained from *fac*-**7** and $ZnBr_2$ in 25% yield after 5 h and in 83% yield after 25 h (Entries 7 and 8 in Table 4). It was found that *fac*-**3** and *fac*-**7** required longer reaction times than those of *fac*-**1** and *fac*-**2** (Entries 5−8 vs Entries 1 and 3 in Table 4). A comparison of

DOI: 10.1021/acs.inorgchem.6b02270
Inorg. Chem. XXXX, XXX, XXX−XXX

Chart 8

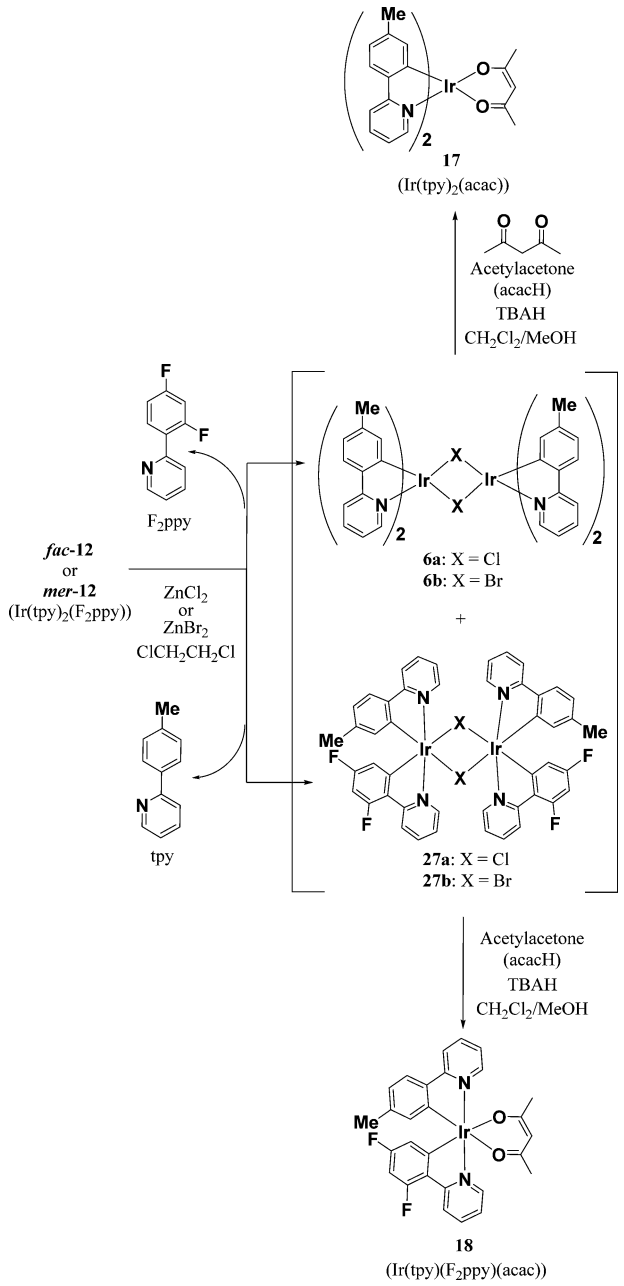

the reactivity between *fac*- and *mer*-forms were inconclusive (Entry 1 vs Entry 2, Entry 3 vs Entry 4 in Table 4 and Entry 1 vs Entry 2 in Table 5). Interestingly, the degradation of ***fac*-8** and ***fac*-9** containing electron-withdrawing groups (two F and NO_2) on the phenyl rings of the ppy ligands negligibly proceeded (Entries 9 and 12 in Table 4), while the *mer*-form of **8** underwent decomposition to give **23b** in 55% (Entry 11). Similarly, ***fac*-11** having CF_3 groups on the phenyl rings had a lower reactivity than that of ***fac*-10** and ***mer*-10** (Entry 3 vs Entries 1 and 2 in Table 5). As shown in Table 2, HCl (4 M in 1,4-dioxane) is a stronger promoter of the degradation reaction than $ZnBr_2$, because the reaction of ***fac*-2** in the presence of HCl proceeds at room temperature, while $ZnBr_2$ requires a refluxing temperature (Entry 4 vs Entry 19 in Table 2). It should be noted that ***fac*-8** and ***fac*-9** have a low reactivity in the presence of HCl/1,4-dioxane under refluxing conditions (Entries 10 and 13 in Table 4) and ***mer*-8** is more reactive than ***fac*-8** (Entry 11 vs Entry 9 in Table 4).

These results indicate that electron-withdrawing groups on the phenyl ring of cyclometalating ligands stabilize the corresponding Ir complexes. From the results shown in Tables 4 and 5, the order of susceptibility to degradation for the ligands against $ZnBr_2$ is assumed to be: mpiq, tpy, and ppy > mppy > Br-tpy > tfpiq > F_2ppy > NO_2-tpy.

Degradation of Tris-Cyclometalated Heteroleptic Ir Complexes in the Presence of Brønsted or Lewis Acids. The aforementioned findings prompted us to examine the ligand-selective degradation of heteroleptic Ir complexes such as *fac*- and *mer*-Ir(tpy)$_2$(F_2ppy) (***fac*-** and ***mer*-12**) by $ZnBr_2$, $ZnCl_2$, TMSCl, $AlCl_3$, and HCl/1,4-dioxane) (Chart 8 and Table 6). Because it was assumed that the degradation of ***fac*-12** and ***mer*-12** with $ZnBr_2$ would likely provide a mixture of **6b** and **27b**, the degradation products were reacted with acacH to convert to **17** (from **6b**) and **18** (from **27b**), respectively, in order to characterize the products more accurately (Chart 8). As shown in Entries 1 and 2 of Table 6, Ir(tpy)$_2$(acac) **17** and Ir(tpy)(F_2ppy)(acac) **18** were obtained in 20% and 40% yields, respectively, from ***fac*-12**, and the chemical yields of **17** and **18** from ***mer*-12** were 13% and 63%, respectively. ^{1}H NMR spectra in Figures S24a and S24b in the Supporting Information support the conclusion that the main products of the reaction of ***mer*-12** with $ZnCl_2$ or $ZnBr_2$ are the corresponding heteroleptic μ-complexes [{Ir(tpy)(F_2ppy)(μ-X)}$_2$] **27a** (X = Cl)[9f] or **27b** (X = Br), respectively.[36] In Entry 3 of Table 6, the crude products containing **6a** and **27a** were reacted with acacH to afford **17** in 6% and **18** in 63% yields. Importantly, **17**, but not **18**, was obtained as a major product of the degradation of

Table 6

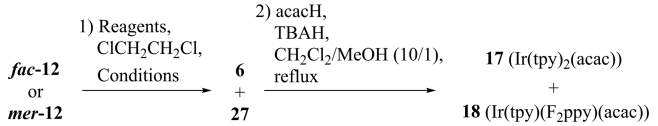

entry	substrates	1) reagents	1) conditions	yield of **17** (%)	yield of **18** (%)	recovery of **12** (%)
1	***fac*-12**	$ZnBr_2$ (50 equiv)	reflux, 20 h	20	40	trace
2	***mer*-12**	$ZnBr_2$ (50 equiv)	reflux, 3 h	13	63	trace
3	***mer*-12**	$ZnCl_2$ (50 equiv)	reflux, 3 h	6	63	trace
4	***mer*-12**	TMSCl (50 equiv)	r.t., 10 min	49	trace	21
5	***mer*-12**	$AlCl_3$ (5.0 equiv)	r.t., 30 min	44	6	29
6	***mer*-12**	HCl (3.0 equiv)[a]	r.t., 1 h	66	trace	15

[a] 4 M HCl in 1,4-dioxane was used.

DOI: 10.1021/acs.inorgchem.6b02270
Inorg. Chem. XXXX, XXX, XXX−XXX

Chart 9

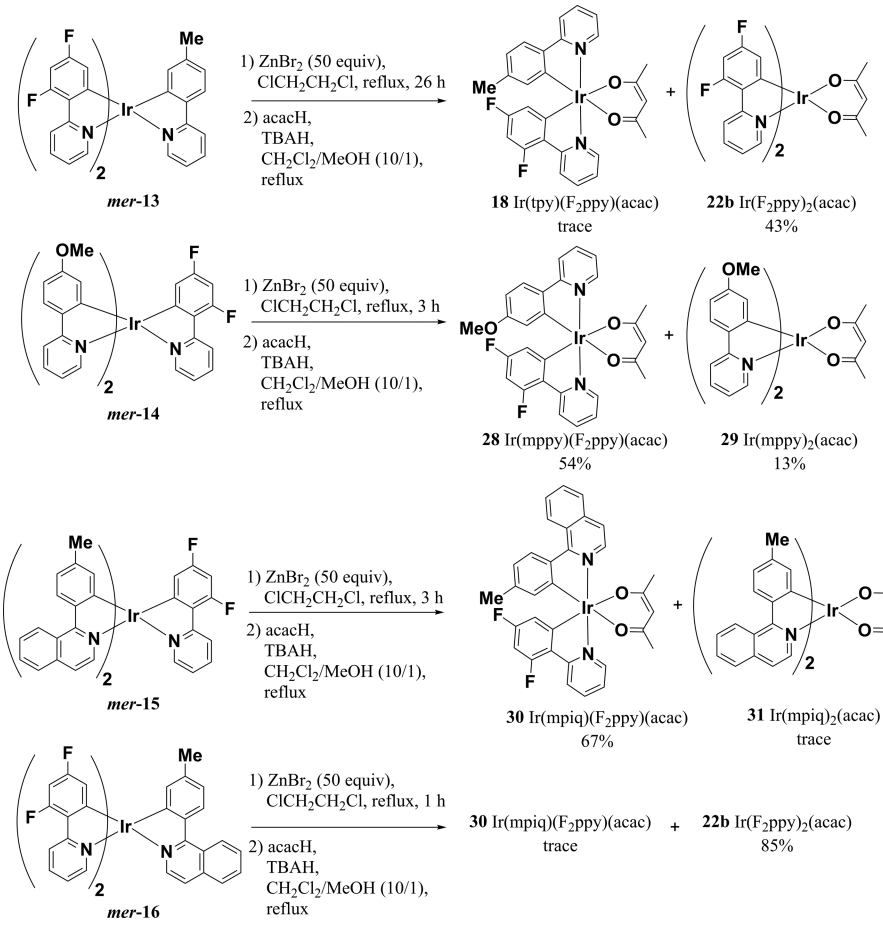

Chart 10

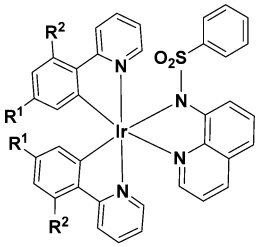

32: $R^1 = R^2 = H$
33: $R^1 = R^2 = F$

***mer*-12** with TMSCl, $AlCl_3$, or HCl (4 M in 1,4-dioxane) (Entries 4–6 in Table 6). The aromatic region in the ^1H NMR spectrum of **18** (obtained from ***fac*-** and ***mer*-12** as a mixture of enantiomers (Δ and Λ forms)) is shown in Figure S25a in the Supporting Information. These results indicate that only ZnX_2 (X = Cl or Br) promotes the selective elimination of a tpy ligand on ***mer*-12**, while TMSCl, $AlCl_3$, and HCl selectively remove the F_2ppy ligand from the same complex.[37]

The ligand-selective degradation reactions by $ZnBr_2$ were further examined using various *mer*-tris-cyclometalated heteroleptic Ir complexes, *mer*-Ir(F_2ppy)$_2$(tpy) (***mer*-13**), *mer*-Ir(mppy)$_2$(F_2ppy) (***mer*-14**), *mer*-Ir(mpiq)$_2$(F_2ppy) (***mer*-15**), and *mer*-Ir(F_2ppy)$_2$(mpiq) (***mer*-16**) (Chart 9). The reaction of ***mer*-13**, which is composed of two F_2ppy ligands and one tpy ligand, with $ZnBr_2$ afforded Ir(F_2ppy)$_2$(acac) **22b** in 43% yield and a trace amount of **18**, implying that the tpy ligand is selectively released from ***mer*-13** under these reaction conditions. The reaction of ***mer*-14** consisting of two mppy and one F_2ppy ligands provided Ir(mppy)(F_2ppy)(acac) **28** in 54% yield and Ir(mppy)$_2$(acac) **29** in 13% yield, as predicted by the higher reactivity of tpy and mppy compared to that of F_2ppy. Similar results were obtained for the reactions of ***mer*-15** and ***mer*-16** with $ZnBr_2$. Namely, Ir(mpiq)(F_2ppy)(acac) **30** and Ir(mpiq)$_2$(acac) **31** were obtained in 67% yield and trace amounts from ***mer*-15**, due to the elimination of the mpiq ligand and **22b** was the major product produced from ***mer*-16**. Aromatic regions of the ^1H NMR spectra of **28** and **30** (obtained from ***mer*-14** and ***mer*-15** as a mixture of enantiomers (Δ and Λ forms)) are shown in Figures S25b and S25c in the Supporting Information in comparison with that of **18** (Figure S25a in the Supporting Information).

We recently reported on the preparation of dual-emissive cyclometalated Ir complexes such as **32** and **33** containing 8BSQ ligand **34** as an ancillary ligand (Chart 10).[19,38] These Ir complexes exhibit two different emission peaks (dual emission) at ca. 475–500 nm (blue to green-color emission) and ca. 600 nm (red-color emission). It was concluded that the F_2ppy unit and the deprotonated 8BSQ group in **32** and **33** contribute to the blue-color emission and red-color emission, respectively, to produce a near-to-white emission.

With the aforementioned method in hand, we synthesized the tris-heteroleptic Ir complexes **35a** and **35b** containing F_2ppy as a blue-emitting ligand, tpy as a green-emitting ligand, and a 8BSQ ligand **34** as a red-emitting ligand. After reacting ***mer*-12** with $ZnBr_2$ or $ZnCl_2$, the resulting μ-complexes were

DOI: 10.1021/acs.inorgchem.6b02270
Inorg. Chem. XXXX, XXX, XXX−XXX

Table 7

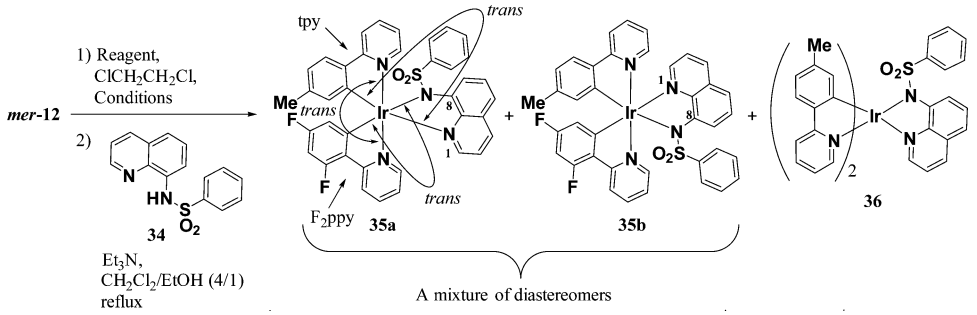

entry	reagents	conditions	yield of **35** (%) (**35a**:**35b**)[a]	yield of **36** (%)
1	$ZnBr_2$ (50 equiv)	reflux, 4 h	36 (1:0.4)	<5
2	$ZnCl_2$ (60 equiv)	reflux, 22 h	24 (1:0.4)	<5
3	TMSCl (60 equiv)	r.t., 10 min	trace	61[c]
4	$AlCl_3$ (5 equiv)	r.t., 10 min	trace	71[c]
5	$FeCl_3$ (5 equiv)	r.t., 10 min	trace	trace
6	HCl (3 equiv)[b]	r.t., 10 min	trace	35[c]

[a]Ratios were determined by ^{1}H NMR. [b]4 M HCl in1,4-dioxane was used. [c]The products were identical to **36** that was prepared according to ref 19.

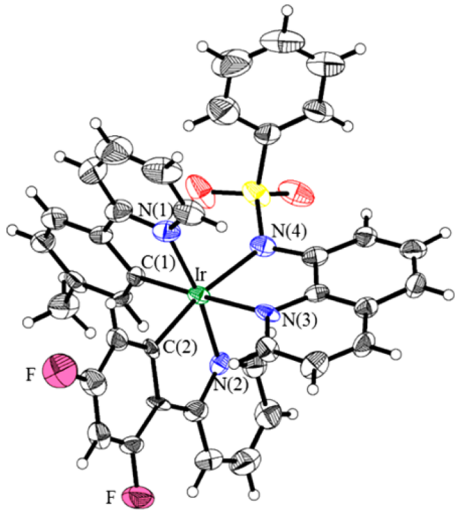

Figure 3. ORTEP drawing of single crystal structure of **35a** with 50% probability ellipsoids.

Table 8. Selected Bond Lengths (Å) of 35a

	bond lengths (Å)
Ir–C(1)	1.99
Ir–C(2)	1.99
Ir–N(1)	2.05
Ir–N(2)	2.04
Ir–N(3)	2.13
Ir–N(4)	2.16

treated with **34** to afford **35** (a mixture of diastereomers **35a** and **35b**) in 36% or 24% yields, respectively, as summarized in Table 7, with a trace amount of **36**. In contrast, **36** was obtained as the major product when TMSCl, $AlCl_3$, or HCl was used (Entries 3, 4, and 6). In Entry 5, treatment with $FeCl_3$ afforded trace amounts of **35** or **36**.

As shown in Figure S26a in the Supporting Information, the ^{1}H NMR spectrum of **35** shows two sets of signals, indicating that it is composed of a mixture of two diastereomers (**35a** and **35b**) in a 1:0.4 ratio, among seven possible diastereomers (the enantiomers of all the diastereomers are not considered). Careful separation of these diastereomers by silica gel column chromatography (hexanes/$CHCl_3$/THF) afforded **35a** as the major product (Figure S26b in the Supporting Information). Its structure was determined by X-ray single crystal analysis, as shown in Figure 3 and Table 8, in which two N atoms in tpy and F_2ppy units connected to Ir atom exhibit *trans* configuration, N(1) of quinolone (N(3) in Figure 3) and C(2) of tpy (C(1) in Figure 3) are *trans*, and NSO_2Ph (N(4) in Figure 3) and C(2) of F_2ppy are also *trans*.[39] To the best of our knowledge, **35a** is the first example of tris-heteroleptic Ir complexes containing a nonsymmetric ancillary ligand isolated as a single stereoisomer (a mixture of Δ and Λ enantiomers).[40]

Mechanistic Study of the Degradation of Ir Complexes Promoted by Brønsted and Lewis Acids. As described above, Baranoff and co-workers reported on the degradation of heteroleptic Ir complexes containing ancillary ligands such as $Ir(F_2ppy)_2$(pic) **22a** and $Ir(F_2ppy)_2$(acac) **22b** with HCl (2 M in Et_2O) and $BF_3{\cdot}Et_2O$ to give the corresponding Ir dimer $[Ir(F_2ppy)_2(\mu\text{-Cl})]_2$ **23a** (Chart 7).[9d]

In contrast, our findings reported herein are that (1) $AlCl_3$, $ZnCl_2$, $ZnBr_2$, TMSCl, and HCl/1,4-dioxane promote the degradation of *tris-cyclometalated Ir complexes* such as ***fac*-2** to afford the corresponding halogen-bridged Ir dimers (Table 2), (2) ***fac*-8**, ***fac*-9**, and ***fac*-11** having electron-withdrawing groups confer a lower reactivity than that of ***fac*-1** and ***fac*-2** (Tables 4 and 5), (3) ZnX_2 (X = Cl or Br) promotes the selective elimination of tpy, mppy, or mpiq ligands from ***fac*-** or ***mer*-12**, ***mer*-14**, and ***mer*-15**, respectively, and the successive reaction with acacH affords heteroleptic Ir complexes that contain three different ligands, such as **18** (Chart 8), **28**, and **30** (Chart 9), while $AlCl_3$, TMSCl, and HCl/1,4-dioxane cause the F_2ppy ligand to be removed from ***mer*-12** (Table 6), (4) the order of reactivity of the *fac*- and *mer*-forms is not conclusive, (5) the order of reactivity of acid promoters is assumed to be HCl/1,4-dioxane, TMSCl, $AlCl_3 \gg ZnX_2$ (Tables 2 and 4), and (6) the optimized structures of ***mer*-13**, ***mer*-14**, and ***mer*-16** were obtained by DFT calculations (Figure S27 in the Supporting Information), because sufficient crystals of these Ir complexes were not obtained for X-ray crystal structure analysis. The Ir–C and Ir–N bond lengths of ***fac*-12**, ***mer*-12**, and ***mer*-15** observed

DOI: 10.1021/acs.inorgchem.6b02270
Inorg. Chem. XXXX, XXX, XXX–XXX

Chart 11

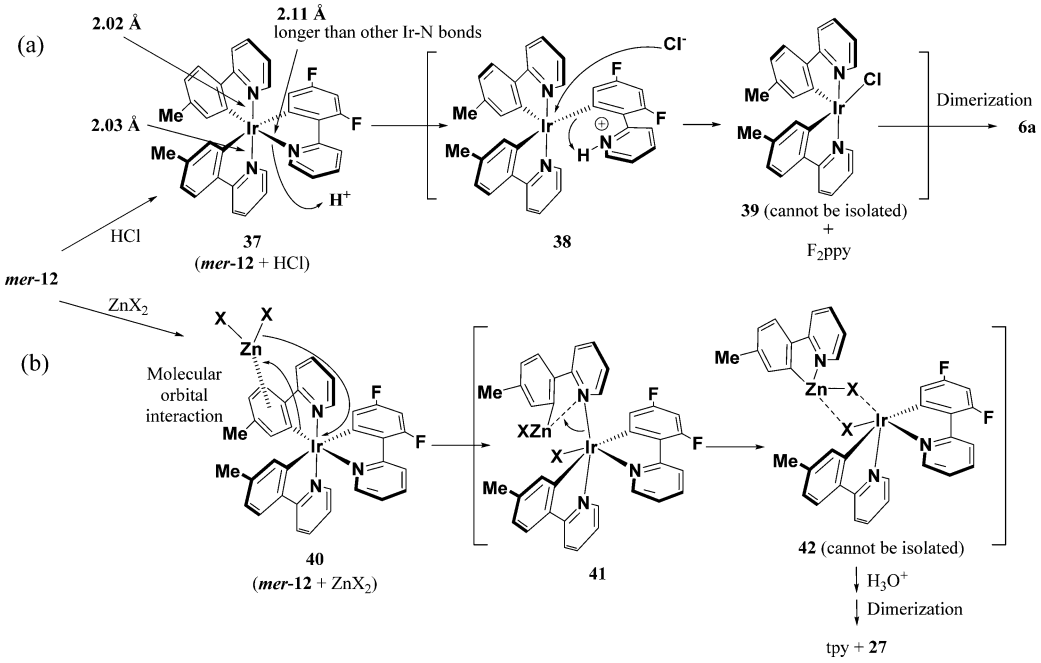

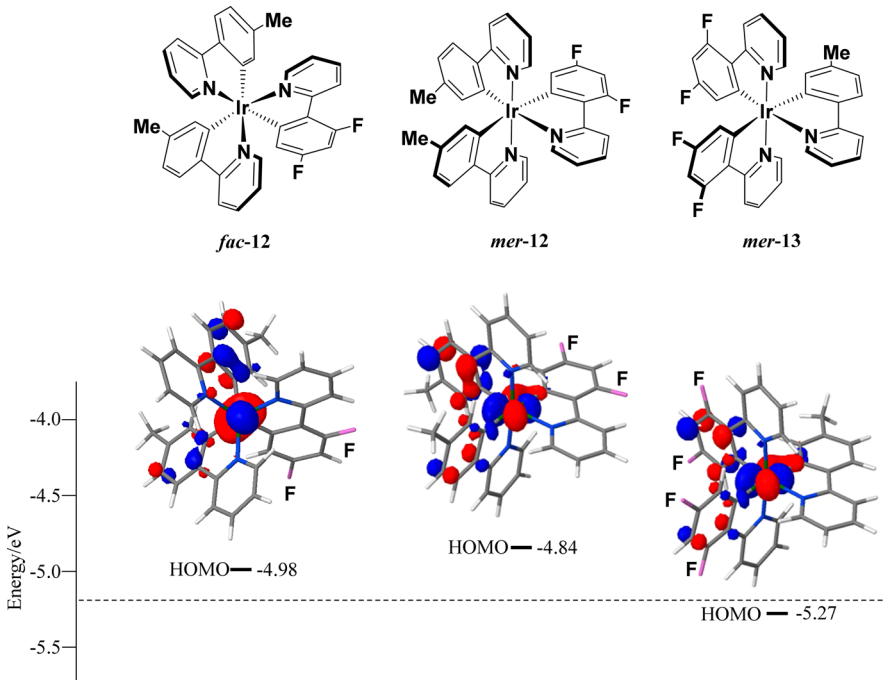

Figure 4. HOMOs of tris-cyclometalated Ir complexes ***fac*-12**, ***mer*-12**, and ***mer*-13** calculated by the Gaussian09 program using the B3LYP hybrid functional together with the LanL2DZ basis for the Ir atom and the 6-31G basis sets for the H, C, N, and F atoms.

Chart 12

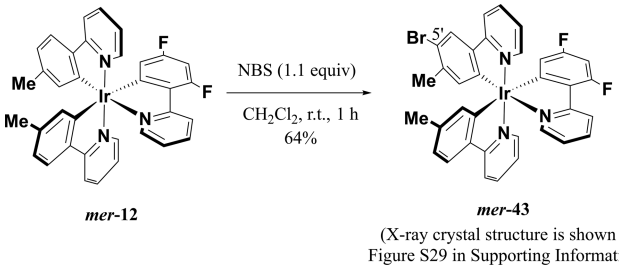

by these crystal structures and those obtained by DFT calculation are nearly identical (Table 1), suggesting that the calculated structures of ***mer*-13**, ***mer*-14**, and ***mer*-16** in Figure S27 in the Supporting Information are sufficiently close to those for the intristic structures (crystal structures, if obtained).

Based on the aforementioned data, we assume two mechanisms for the degradation of tris-cyclometalated Ir complexes (typically, ***mer*-12**) according to the used acids, as shown in Chart 11. In hard and soft acids and bases (HSAB) theory, H^+, Al^{3+}, and Si^{4+} are categorized as hard Lewis acids and Zn^{2+} is categorized as borderline acids.[41] When H^+, $AlCl_3$,

DOI: 10.1021/acs.inorgchem.6b02270
Inorg. Chem. XXXX, XXX, XXX−XXX

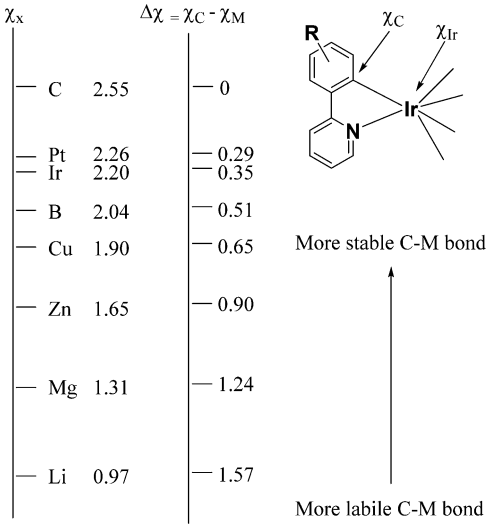

Figure 5. Electronegativity values for carbon and several metals.

or TMSCl are used for the degradation, the nitrogen atom on the F_2ppy ligand in the ***mer*-12** reacts with H^+, Al^{3+} (of $AlCl_3$), or Si^{4+} (of TMSCl), which are hard acids (**37**), resulting in the formation of the intermediate **39** via **38** (Chart 11a). This can be attributed to the fact that the Ir−N bond of F_2ppy is longer (namely weaker) than the other Ir−N bonds between Ir and the tpy ligand (Table 1b). Cleavage of the Ir−C bond of **38** affords **39**, which may easily dimerize to give **6a**.

In the case of Zn^{2+}-promoted degradation reactions, on the other hand, we hypothesize an interaction between the molecular orbital of the phenyl ring of ***mer*-12** and that of Zn^{2+} (**40** in Chart 11b), because Zn^{2+} is one of the borderline acids. This reaction is considered to initiate the metal exchange reaction from Ir−C to Zn−C to give the intermediate **42** via **41**, resulting in the production of **27** and tpy (30−70%) (Entries 3 and 4 in Table 2 and Entries 2 and 3 in Table 6).

The decomposition reaction of ***fac*-2** with ZnX_2 (X = Cl or Br) was carried out in the presence of aldehyde to trap the Zn^{2+}-coordinated species such as **42**. It was hypothesized that Reformatsky reagent-like species in **42** (Chart 11) may undergo C−C bond formation reaction with benzaldehyde, considering an analogy to the nucleophilic C(sp^2)−H addition of manganase reagents to aldehyde, as reported by Wang and co-workers.[42] In a typical experiment, a solution of benzaldehyde in THF was added to a degradation reaction mixture of ***fac*-2** and $ZnBr_2$ after cooling to room temperature. It should be noted that THF was used as a cosolvent to dissociate **42** and activate organozinc species in it. In this reaction, however, **6b** was obtained in 53% and benzaldehyde was recovered in 73%. After the decomposition in the presence of *p*-nitrobenzaldehyde, ***fac*-2** was recovered in 58% and a complex mixture was obtained.

Next, we carried out the quenching experiments of the Zn^{2+}-promoted degradation reaction with D_2O/DCl or MeOD to check the formation of the deuterated tpy ligand. The reaction mixture of ***fac*-2** and $ZnCl_2$ was refluxed for 2 h, to which D_2O/DCl or MeOD was added and refluxed again for 30 min. In these experiments, tpy was recovered in 30−70% without substitution with deuterium (D). Futhermore, the degradation of ***fac*-2** with $ZnCl_2$ in 1,2-dichloroethane-d_4 ($ClCD_2CD_2Cl$) gave tpy in 28% without deuteriumation, denying that 1,2-dichloroethane functions as a proton donor to **42**. These experimental results suggest that a very small amount of H_2O contained in ZnX_2 may function as a proton donor to the organozinc species in **42**. Further study is now in progress.

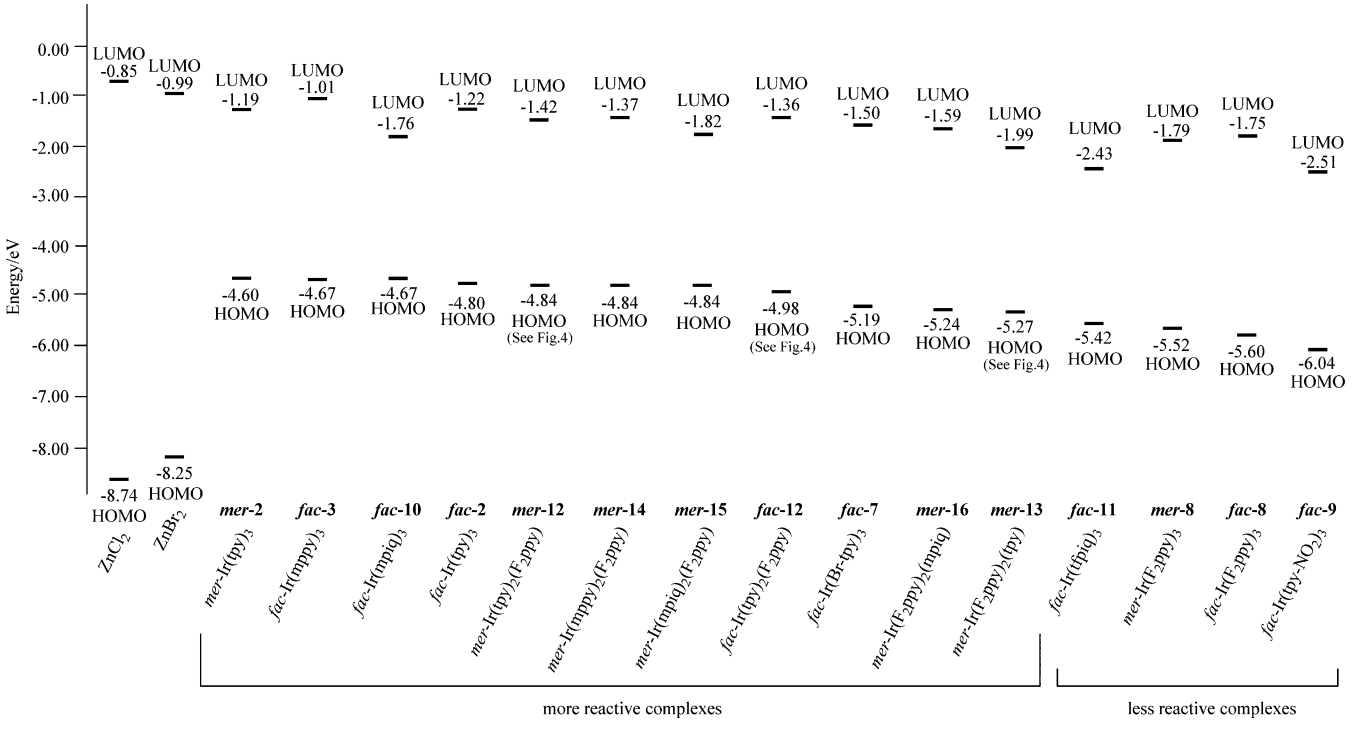

Figure 6. Energy diagram for the HOMO and LUMO of tris-cyclomatalated Ir complexes (***fac*-2**, ***mer*-2**, ***fac*-3**, ***fac*-7**, ***fac*-8**, ***mer*-8**, ***fac*-9**, ***fac*-10**, ***fac*-11**, ***fac*-12**, and ***mer*-12−16**), $ZnCl_2$, and $ZnBr_2$ calculated by the Gaussioan09 program using the B3LYP hybrid functional together with the LanL2DZ basis for the Ir, Zn, Cl, and Br atoms and the 6-31G basis sets for the H, C, N, O, and F atoms.

DOI: 10.1021/acs.inorgchem.6b02270
Inorg. Chem. XXXX, XXX, XXX−XXX

Table 9. Photophysical Properties of *mer*-10, *mer*-12−16, *fac*-12, 17, 18, 22b, and 28−31 in Degassed DMSO Solutions at 298 K[a]

compounds	λ_{abs} (nm)	λ_{em} (nm)	quantum yield Φ	emission lifetime τ (μs)
***mer*-10** (*mer*-Ir(mpiq)$_3$)	303, 350, 486	614	2.0×10^{-2}[b]	0.17[d]
***fac*-12** (*fac*-Ir(tpy)$_2$(F$_2$ppy))	281, 362	516	0.57[c]	1.9[e]
***mer*-12** (*mer*-Ir(tpy)$_2$(F$_2$ppy))	336, 366, 400	528	4.7×10^{-2}[c]	0.30[f]
***mer*-13** (*mer*-Ir(F$_2$ppy)$_2$(tpy))	278, 389	504	0.31[c]	1.0[e]
***mer*-14** (*mer*-Ir(mppy)$_2$(F$_2$ppy))	278, 409	512	8.3×10^{-2}[c]	0.25[e]
***mer*-15** (*mer*-Ir(mpiq)$_2$(F$_2$ppy))	281, 343, 470	603	0.22[b]	1.1[d]
***mer*-16** (*mer*-Ir(F$_2$ppy)$_2$(mpiq))	272, 354, 395	581	0.31[b]	4.7[g]
17 (Ir(tpy)$_2$(acac))	408, 462	518	0.42[c]	1.4[e]
18 (Ir(tpy)(F$_2$ppy)(acac))	400, 450	508	0.51[c]	1.3[e]
22b (Ir(F$_2$ppy)$_2$(acac))	330, 389, 437	489	0.53[c]	1.0[e]
28 (Ir(mppy)(F$_2$ppy)(acac))	283, 395, 472	507	0.52[c]	1.3[e]
29 (Ir(mppy)$_2$(acac))	286, 401	505	0.46[c]	1.2[e]
30 (Ir(mpiq)(F$_2$ppy)(acac))	280, 340, 455	493, 602	0.38[b]	1.9,[e] 2.0[d]
31 (Ir(mpiq)$_2$(acac))	289, 345, 474	616	0.25[b]	1.3[d]

[a]Excitation at 366 nm; [Ir complex] = 10 μM. [b]Quantum yields were determined using *fac*-Ir(mpiq)$_3$ as a standard reference (Φ = 0.26 in toluene). [c]Quantum yields were determined using quinine sulfate as a standard reference (Φ = 0.55 in 0.1 M H_2SO_4 aq.). [d]A 590 nm long wave pass filter was used. [e]A 475 nm long wave pass filter was used. [f]A 515 nm long wave pass filter was used. [g]A 550 nm long wave pass filter was used.

The energy levels and shapes of HOMO of ***fac*-12**, ***mer*-12**, and ***mer*-13** are presented in Figure 4. The same parameters of ***mer*-14**, ***mer*-15**, and ***mer*-16** are shown in Figure S28 in the Supporting Information. The successive cleavage of Ir−N may afford **42**, which could exist as a hetero μ-complex between them (**41**) and are then decomposed to tpy and **27b** after quenching.

In support of the reactivity of their phenyl groups, the treatment of ***mer*-12** with NBS afforded ***mer*-43**, whose 5′-position is brominated (Chart 12),[10,11] as confirmed by X-ray structure (Figure S29 in the Supporting Information). Note that ***mer*-43** is, to the best of our knowledge, the first example of *tris-heteroleptic tris-cyclometalated Ir complex* that is synthesized without the formation of other diastereomers. As shown in Figure 2, two Ir atoms in **6a** have *N,N-trans* configuration and the same product **6a** is obtained from ***fac*-12** and ***mer*-12**, in which Ir has *N,N-cis* configuration and *N,N-trans* configuration, although this mechanism is yet to be studied.

The data in Table 4 indicate, that ***fac*-8** and ***fac*-9**, which include the electron-withdrawing groups, have lower reactivity in the presence of ZnX_2 and HCl. For reference, it has been reported that the bonds between metal (M) and the oxygen atom of the M(8-hydroxyquinolyl)$_3$ complex (M = Al(III) or In (III)) are stabilized by the introduction of Br and NO_2 groups on the 8-hydroxyquinolyl ligand.[43] We then asked ourselves why Ir complexes having electron-withdrawing groups such as ***fac*-8**, ***fac*-9**, and ***fac*-11** are less reactive than ***fac*-1** and ***fac*-2**.

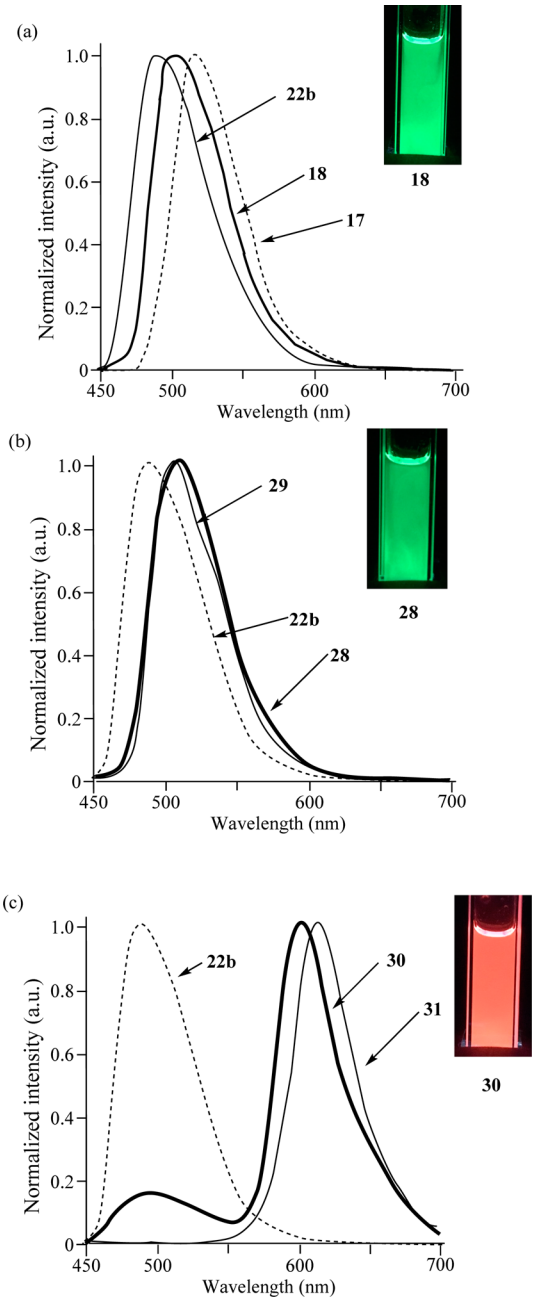

Figure 7. Normalized emission spectra of Ir complexes. (a) **17** (dashed curve), **18** (bold curve), and **22b** (plain curve) in degassed DMSO at 298 K ([Ir complex] = 10 μM and excitation at 366 nm). (inset) Photograph showing DMSO solution of **18** (10 μM) excited by UV light at 365 nm. (b) **22b** (dashed curve), **28** (bold curve), and **29** (plain curve). (inset) Photograph showing DMSO solution of **28** (10 μM) excited by UV light at 365 nm. (c) **22b** (dashed curve), **30** (bold curve), and **31** (plain curve). (inset) Photograph showing DMSO solution of **30** (10 μM) excited by UV light at 365 nm.

It is well described that Ir complexes are one of most kinetically inert class of metal complexes[44] and the significant stability of cyclometalated Ir complexes in comparison with organometallic reagents such as organolithium and organomagnesium reagents can be explained by the difference of electronegativity of the carbon (χ_c) and the corresponding metals (χ_{Ir}, χ_{Li}, and χ_{Mg}).[45] The electronegativity values for carbon and iridium are 2.55 (χ_c) and 2.20 (χ_{Ir}), respectively, from which the $\Delta\chi$ value between C and Ir is calculated to be

DOI: 10.1021/acs.inorgchem.6b02270
Inorg. Chem. XXXX, XXX, XXX−XXX

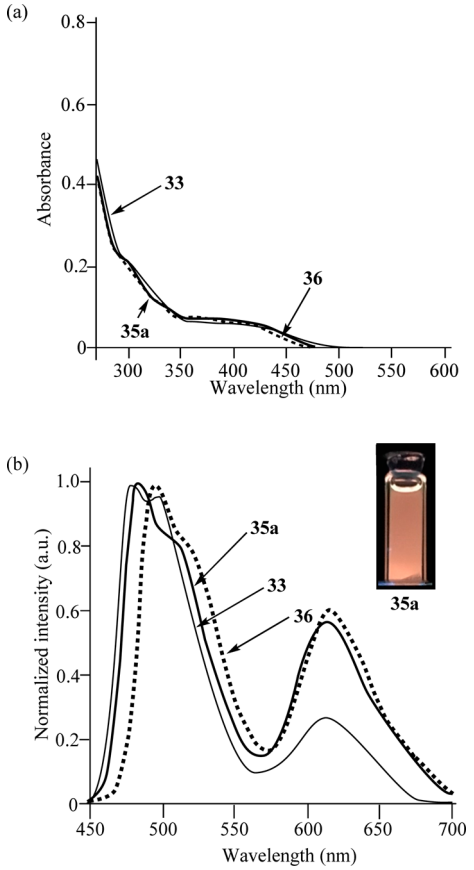

Figure 8. (a) UV/vis spectra of Ir complexes **33** (plain curve), **35a** (bold curve), and **36** (dashed bold curve) in DMSO at 298 K. (b) Normalized emission spectra of **33** (plain curve), **35a** (bold curve), **36** (dashed bold curve) in degassed DMSO at 298 K ([Ir complex] = 10 μM and excitation at 366 nm). (inset) Photograph showing DMSO solution of **35a** (10 μM) excited by UV light at 365 nm.

Table 10. Photophysical Properties of 33, 35a, and 36 in Degassed DMSO Solutions at 298 K[a]

		λ_{em} (nm)			
compounds	λ_{abs} (nm)	HEB[b]	LEB[b]	quantum yield (Φ)	emission lifetime τ (μs)
33	331, 366, 417	474, 493	613	9.8×10^{-2}	1.4, 9.3[c]
35a	299, 381, 424	485, 515	613	2.5×10^{-2}	1.9, 13[d]
36	304, 335, 386, 446	497, 525	617	1.5×10^{-2}	1.6, 10[d]

[a]Excitation at 366 nm; [Ir complex] = 10 μM). [b]HEB = higher energy emission band, LEB = lower energy emission band. [c]A 435 nm long wave pass filter was used. [d]A 475 nm long wave pass filter was used.

0.35, as displayed in Figure 5. This value is smaller than the corresponding values for reactive organometallic reagents like organolithium, organomagnesium, and organozinc reagents, which explains the higher stability of C−Ir bonds in Ir complexes in comparison with C−Li, C−Mg, and C−Zn bonds. It is possible that electron-withdrawing groups (R in Figure 5) on the phenyl rings of ***fac*-8**, ***mer*-8**, ***fac*-9**, and ***fac*-11** (Tables 4 and 5) would decrease the electronegativity of carbon atoms in Ir−C bonds indicated in Figure 5, resulting in a decrease in the $\Delta\chi$ value and the higher stability of these complexes compared to ***fac*-1** and ***fac*-2**.

The HOMO and LUMO energy levels of the Ir complexes were also considered. Figure 6 provides information on the HOMO and LUMO levels of the Ir complexes used in the decomposition reactions. In the left half of Figure 6, the HOMO and LUMO levels of the more reactive Ir complexes are shown and the less reactive complexes are listed in the right half.[46] We next focused on the relationship between HOMO levels of Ir complexes and LUMO levels of $ZnBr_2$. Among the reactive Ir complexes, ***mer*-13** (*mer*-Ir(F_2ppy)$_2$(tpy)) has the most negative HOMO level (−5.27 eV) and the less reactive Ir complexes (e.g.; **8** and **9**) possess more negative HOMO levels (<−5.4 eV).

The LUMO level of the optimized structure of $ZnBr_2$ is estimated to be ca. −1 eV by DFT calculation (B3LYP/LanL2DZ). Thus, we assume that orbital interactions between the LUMO of $ZnBr_2$ (ca. −1 eV) and the HOMOs (more positive than ca. −5.2 eV) of the Ir complexes are important for these degradation reactions. LUMO energy level of $ZnBr_2$ (−0.99 eV) is lower than that of $ZnCl_2$ (−0.85 eV) and we assume that this is the reason why higher yield was obtained in the decomposition of ***fac*-2** with $ZnBr_2$ than that with $ZnCl_2$. At the same time, ZnX_2 functions as a halide source to afford μ-complex.

Regarding the mechanism of the selective-degradation reaction of *mer*-tris-cyclometalated heteroleptic Ir complexes such as ***fac*-12**, ***mer*-12**, and ***mer*-13** promoted by $ZnBr_2$ (Charts 8 and 9), the HOMOs of these complexes are located on the major ligand in each complex (Figure 4). Namely, ***mer*-12** and ***fac*-12** contain two tpy and one F_2ppy ligands and its HOMO is located on tpy as well as the Ir metal core. ***Mer*-13** includes two F_2ppy and one tpy groups and its HOMO is located on the F_2ppy unit and the Ir core. Therefore, we assume that the HOMO on tpy ligands in **12** and that on the F_2ppy of **13** interact with the LUMO of $ZnBr_2$, as speculated in **40** of Chart 11b, thus initiating the selective decomposition of the corresponding ligand (similarly, the HOMOs of ***mer*-14**, ***mer*-15**, and ***mer*-16** are shown in Figure S28 in the Supporting Information, in which similar behavior is observed). It should be noted that ***mer*-13** and ***mer*-16** are exceptions, from which the minor ligand (tpy or mpiq) is ejected faster than the major ligand (F_2ppy).

Photophysical Properties of the Ir Complexes. UV/vis absorption spectra of ***mer*-10**, ***mer*-12−16**, ***fac*-12**, **17**, **18**, **22b**, and **28−31** (10 μM) in DMSO at 298 K are shown in Figure S30 in the Supporting Information, and their photochemical properties are summarized in Table 9. These complexes exhibit a weak absorption in the region of *ca.* 350−500 nm, which are due to spin-allowed and spin-forbidden metal-to-ligand change transfer (MLCT) transitions and spin-forbidden $\pi-\pi^*$ transitions.

Emission spectra of the substrates of degradation, ***mer*-10**, ***mer*-12−16**, ***fac*-12**, and products obtained in this work, **17**, **18**, **22b**, and **28−31** (10 μM in degassed DMSO), were measured at 298 K (excitation at 366 nm), as shown in Figure S31 in the Supporting Information and Figure 7, respectively, and their quantum yields were determined based on the Φ value of quinine sulfate in 0.1 M H_2SO_4 (Φ = 0.55) or *fac*-Ir(mpiq)$_3$ in toluene (Φ = 0.26) used as a standard reference (see Table 9).[47] The emission maxima of **17**, **18**, and **22b** are 518, 508, and 489 nm, respectively, indicating that the emission maxima of tris-heteroleptic Ir complex **18** is located between those of **17** and **22b**. As expected, it was found that **30** exhibits a dual emission at ca. 493 nm and ca. 602 nm, respectively, because

DOI: 10.1021/acs.inorgchem.6b02270
Inorg. Chem. XXXX, XXX, XXX−XXX

Table 11. Calculated Triplet Transition States and Characteristics of the Transitions of 30 and 35a Using TD-DFT Calculation at B3LYP (the LANL2DZ/6-31G Level)

compound	λ_{em} (nm) exp	E (eV) exp	E (eV) TD-DFT	state	assignment	main transition character[a]
30	602	2.06	1.91	T_1	HOMO − 2 → LUMO (17%) HOMO − 1 → LUMO (8%) HOMO → LUMO (69%)	$^3ML_{mpiq}CT + {}^3L_{mpiq}C + {}^3L_{acac}L_{mpiq}CT$
			2.40	T_2	HOMO − 2 → LUMO (23%) HOMO − 1 → LUMO (42%) HOMO → LUMO (25%)	$^3ML_{mpiq}CT + {}^3L_{mpiq}C + {}^3L_{acac}L_{mpiq}CT$
	493	2.52	2.57	T_3	HOMO − 1 → LUMO + 1 (6%) HOMO → LUMO + 1 (79%)	$^3ML_{F2ppy}CT + {}^3L_{mpiq}L_{F2ppy}CT + {}^3L_{acac}L_{F2ppy}CT$
35a	613	2.02	1.94	T_1	HOMO − 1 → LUMO (13%) HOMO → LUMO (79%)	$^3ML_{quin}CT + {}^3L_{quin}C + {}^3IL_{quin}CT + {}^3L_{tpy}L_{quin}CT$
	485	2.56	2.59	T_2	HOMO − 2 → LUMO + 2 (11%) HOMO − 1 → LUMO + 1 (4%) HOMO − 1 → LUMO + 2 (33%) HOMO → LUMO + 1 (6%) HOMO → LUMO + 2 (34%)	$^3ML_{tpy}CT + {}^3ML_{F2ppy}CT + {}^3L_{tpy}C + {}^3L_{tpy}L_{F2ppy}CT + {}^3L_{quin}L_{tpy}CT + {}^3L_{quin}L_{F2ppy}CT$

[a]The metal-to-ligand charge transfer, interligand charge transfer, intraligand charge transfer, and ligand centered are represented by ML_xCT, L_xL_yCT, IL_xCT, and LC_x, respectively. quin: quinoline ligand.

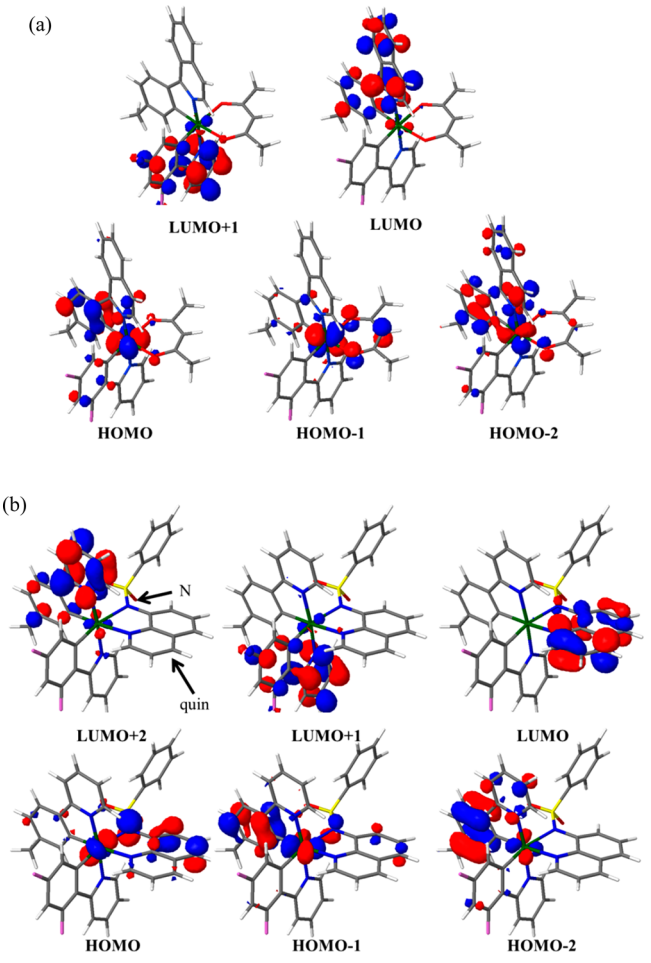

Figure 9. Selected molecular orbitals of (a) **30** and (b) **35a** obtained from DFT calculations at B3LYP (the LANL2DZ/6-31G level).

the F_2ppy and mpiq ligands emit a blue and a red color, respectively. It should be noted that **30** was recrystallized twice in order to minimize contamination by **22b** and **31** and the exactly the same spectra were observed after recrystallization.

The UV/vis absorption spectra and emission spectra of **33**, **35a**, and **36** (10 μM in degassed DMSO solutions at 298 K) are shown in Figure 8, and their photochemical properties are summarized in Table 10. These complexes also exhibited a weak absorption in the region of ca. 350−530 nm, which are due to spin-allowed and spin-forbidden metal−ligand charge transfer (MLCT) transitions and spin-forbidden $\pi-\pi^*$ transitions.

Since these Ir complexes contain 8BSQ ligand as an ancillary ligand, they exhibit dual emissions at ca. 475−525 nm (HE (high energy) emission band) and ca. 610 nm (LE (low energy) emission band) ($\Phi = 2.5 \times 10^{-2}$ for **35a**, 9.8×10^{-2} for **33**, and 1.5×10^{-2} for **36**; Figure 8b and Table 10).[19] The maxima of HEB of **35a** was found to be observed between those of **36** and **33**. As shown in the inset of Figure 8b, **35a** exhibits a pale-pink emission color. The CIE of representative Ir complexes synthesized in this work is presented in Figure S32 in the Supporting Information.

Mechanistic Studies of Dual Emission of Ir complexes (30 and 35a). TD-DFT calculations were performed for **30** and **35a** using the Gaussian09 program.[13] For **30**, the calculated triplet energies T_1 and T_3 are close to the experimentally determined values (T_1 2.06 eV (602 nm) and T_3 2.52 eV (493 nm); Table 11). The HOMO and HOMO−2 of **30** are mainly localized on the Ir center and mpiq ligands and HOMO−1 is mainly localized on the Ir centers and acac ligands, as shown in Figure 9a. The LUMO and LUMO+1 are localized on the mpiq and F_2ppy ligands, respectively. TD-DFT calculations show that $^3ML_{mpiq}CT$ ($d(\pi)(Ir) \rightarrow \pi^*(mpiq)$), $^3L_{mpiq}C$ ($\pi(mpiq) \rightarrow \pi^*(mpiq)$), and $^3L_{acac}L_{mpiq}CT$ transitions ($\pi(acac) \rightarrow \pi^*$-(mpiq)) (Table 11) are included in the lowest-energy triplet excited state T_1. The third lowest-energy state T_3 of **30** is identical to its experimentally determined HEB, indicating that

DOI: 10.1021/acs.inorgchem.6b02270
Inorg. Chem. XXXX, XXX, XXX−XXX

T_3 is a mixture of $^3ML_{F2ppy}CT$ (d(π)(Ir) → π^*(F_2ppy)), $^3L_{mpiq}L_{F2ppy}CT$ (π(mpiq) → π^*(F_2ppy)), and $^3L_{acac}L_{F2ppy}CT$ transitions (π(acac) → π^*(F_2ppy)).

The calculated triplet energies T_1 and T_2 of **35a** were 1.94 and 2.59 eV, respectively, which are in fairly good agreement with the experimentally determined values (T_1: 2.02 eV (613 nm) and T_2: 2.56 eV (485 nm). As shown in Figure 9b, the HOMO of **35a** is mainly localized on the Ir center, the quinoline ring (quin), and the nitrogen atom (n) of the sulfonamide group of quinoline, and the HOMO−1 and HOMO−2 are mainly localized on the Ir centers and tpy ligands. On the other hand, its LUMO is localized on the quinoline ring, and LUMO+1 and LUMO+2 are mainly localized on the F_2ppy and tpy ligands, respectively. The results of TD-DFT calculations suggest that the lowest-energy triplet excited state T_1 is a mixture of $^3ML_{quin}CT$ (d(π)(Ir) → π^*(quin)), $^3L_{quin}C$ (π(quin) → π^*(quin)), $^3IL_{quin}CT$ (n-(sulfonamide) → π^*(quin)), and $^3L_{tpy}L_{quin}CT$ transitions (π(tpy) → π^*(quin)) (Table 11). Furthermore, the second lowest-energy state T_2 of **35a** is a mixture of $^3ML_{tpy}CT$ (d(π)(Ir) → π^*(tpy)), $^3ML_{F2ppy}CT$ (d(π)(Ir) → π^*(F_2ppy)), $^3L_{tpy}C$ (π(tpy) → π^*(tpy)), $^3L_{tpy}L_{F2ppy}CT$ (π(tpy) → π^*-(F_2ppy)), $^3L_{quin}L_{tpy}CT$ (π(quin) → π^*(tpy)), and $^3L_{quin}L_{F2ppy}CT$ transitions (π(quin) → π^*(F_2ppy)). These results indicate the contribution of each of the three different ligands (F^2ppy, tpy, and 8BSQ) to the triplet emission states of **35a**.

CONCLUSION

In this manuscript, we report on the degradation of tris-cyclometalated Ir complexes (IrL_3, L = cyclometalating ligand) promoted by Brønsted acids such as HCl/1,4-dioxane and Lewis acids such as ZnX_2 (X = Br or Cl), TMSCl, and $AlCl_3$. Among the various Lewis acids, $ZnBr_2$ exhibited a good reactivity for Ir(ppy)$_3$ **1**, Ir(tpy)$_3$ **2**, and Ir(mppy)$_3$ **3** to provide the corresponding halogen-bridged Ir dimers (μ-complexes). It was also found that the reactivity of tris-cyclometalated Ir complexes containing electron-withdrawing groups such as fluorine atoms, nitro or CF_3 groups on the ligands is quite low. This reaction was applied to the selective degradation of *mer*-tris-cyclometalated Ir complexes such as *mer*-Ir(tpy)$_2$(F_2ppy) (***mer*-12**). The reaction of ***mer*-12** with $ZnBr_2$ gave a mixture of a halogen-bridged Ir dimer **6b** and **27b**, and the tris-heteroleptic Ir complex **18** (IrLL′A, A = ancillary ligand) was then obtained by treatment with acetylacetone. Furthermore, we successfully isolated a novel tris-heteroleptic Ir complex **35a** having a nonsymmetric ancillary ligand after careful separation of its diastereomers. Mechanistic studies suggest that the formation of different products from some Ir complexes by H^+, TMSCl, and $AlCl_3$ and ZnX_2 is due to the hardness and softness of these Brønsted and Lewis acids used. The reactivity and selectivity in the ZnX_2-promoted degradation can be explained by the interaction of the HOMO of Ir complexes with the LUMO of ZnX_2 and by the difference of electronegativity of iridium and carbon in the ligand part. Further mechanistic study is now underway. Such selective degradation reactions of tris-cyclometalated Ir complexes represents a potentially useful synthetic method for preparing a variety of metal complexes.

ASSOCIATED CONTENT

Supporting Information

The Supporting Information is available free of charge on the ACS Publications website at DOI: 10.1021/acs.inorgchem.6b02270.

Chart S1, Figures S1-S32, and Table S1 as mentioned in the text (PDF)
Rotatable crystallographic information for **6a** (CIF)
Rotatable crystallographic information for ***fac*-12** (CIF)
Rotatable crystallographic information for ***mer*-12** (CIF)
Rotatable crystallographic information for ***mer*-15** (CIF)
Rotatable crystallographic information for **35a** (CIF)
Rotatable crystallographic information for ***mer*-43** (CIF)

AUTHOR INFORMATION

Corresponding Author

*E-mail: shinaoki@rs.noda.tus.ac.jp. Phone no.: +81-4-7121-3670.

ORCID

Shin Aoki: 0000-0002-4287-6487

Notes

The authors declare no competing financial interest.

ACKNOWLEDGMENTS

This work is supported by the Grants-in-Aid from the Ministry of Education, Culture, Sports, Science, and Technology (MEXT) of Japan (Nos. 26860016 and 16K18851 for Y.H. and Nos. 24659055 and 24640156 for S.A.), the Uehara Memorial Foundation for Y.H., TUS (Tokyo University of Science) fund for strategic research areas, and "Academic Frontier" project for private universities: matching fund subsidy from MEXT. We wish to acknowledge Dr. Miho Hatanaka (Faculty of Science and Technology, Kindai University) for helpful discussion about degradation mechanism and Mrs. Fukiko Hasegawa (Faculty of Pharmaceutical Science, Tokyo University of Science) for measurement of the mass spectra. We appreciate the aid of Dr. Kenji Yoza (Bruker AXS) and Ms. Tomoko Mastsuo (Research Institute for Science of Technology, Tokyo University of Science) for the X-ray single crystal structure analysis. We thank Ms. Kana Naito and Ms. Aya Kando for the preparation of some compounds.

REFERENCES

(1) (a) Maity, A.; Anderson, B. L.; Deligonul, N.; Gray, T. G. Room-Temperature Synthesis of Cyclometalated Iridium(III) Complexes: Kinetic Isomers and Reactive Functionalities. *Chem. Sci.* **2013**, *4*, 1175−1181. (b) Fernández-Hernández, J. M.; Yang, C. H.; Beltran, J. I.; Lemaur, V.; Polo, F.; Frohlich, R.; Cornil, J.; De Cola, L. Control of the Mutual Arrangement of Cyclometalated Ligands in Cationic Iridium(III) Complexes. Synthesis, Spectroscopy, and Electroluminescence of the Different Isomers. *J. Am. Chem. Soc.* **2011**, *133*, 10543−10558. (c) Aubert, V.; Ordronneau, L.; Escadeillas, M.; Williams, J. A. G.; Boucekkine, A.; Coulaud, E.; Dragonetti, C.; Righetto, S.; Roberto, D.; Ugo, R.; Valore, A.; Singh, A.; Zyss, J.; Ledoux-Rak, I.; Le Bozec, H.; Guerchais, V. Linear and Nonlinear Optical Properties of Cationic Bipyridyl Iridium(III) Complexes: Tunable and Photoswitchable? *Inorg. Chem.* **2011**, *50*, 5027−5038. (d) Valore, A.; Colombo, A.; Dragonetti, C.; Righetto, S.; Roberto, D.; Ugo, R.; De Angelis, F.; Fantacci, S. Luminescent Cyclometallated Ir(III) and Pt(II) Complexes with β-Diketonate Ligands as Highly Active Second-Order NLO Chromophores. *Chem. Commun.* **2010**, *46*, 2414−2416. (e) Dragonetti, C.; Falciola, L.; Mussini, P.; Righetto, S.; Roberto, D.; Ugo, R.; Valore, A.; De Angelis, F.; Fantacci, S.;

DOI: 10.1021/acs.inorgchem.6b02270
Inorg. Chem. XXXX, XXX, XXX−XXX

Sgamellotti, A.; Ramon, M.; Muccini, M. The Role of Substituents on Functionalized 1,10-Phenanthroline in Controlling the Emission Properties of Cationic Iridium(III) Complexes of Interest for Electroluminescent Devices. *Inorg. Chem.* **2007**, *46*, 8533−8547. (f) Dragonetti, C.; Righetto, S.; Roberto, D.; Ugo, R.; Valore, A.; Fantacci, S.; Sgamellotti, A.; De Angelis, F. Cyclometallated Iridium-(III) Complexes with Substituted 1,10-Phenanthrolines: A New Class of Highly Active Organometallic Second Order NLO-Phores with Excellent Transparency with Respect to Second Harmonic Emission. *Chem. Commun.* **2007**, 4116−4118. (g) Huo, S.; Deaton, J. C.; Rajeswaran, M.; Lenhart, W. C. Highly Efficient, Selective, and General Method for the Preparation of Meridional Homo- and Heteroleptic Tris-Cyclometalated Iridium Complexes. *Inorg. Chem.* **2006**, *45*, 3155−3157. (h) Tamayo, A. B.; Alleyne, B. D.; Djurovich, P. I.; Lamansky, S.; Tsyba, I.; Ho, N. N.; Bau, R.; Thompson, M. E. Synthesis and Characterization of Facial and Meridional Tris-Cyclometalated Iridium(III) Complexes. *J. Am. Chem. Soc.* **2003**, *125*, 7377−7387. (i) Obara, S.; Itabashi, M.; Okuda, F.; Tamaki, S.; Tanabe, Y.; Ishii, Y.; Nozaki, K.; Haga, M. Highly Phosphorescent Iridium Complexes Containing Both Tridentate Bis(Benzimidazolyl)-Benzene or -Pyridine and Bidentate Phenylpyridine: Synthesis, Photophysical Properties, and Theoretical Study of Ir-Bis-(Benzimidazolyl)Benzene Complex. *Inorg. Chem.* **2006**, *45*, 8907−8921.

(2) (a) Omae, I. Application of the Five-Membered Ring Blue Light-Emitting Iridium Products of Cyclometalation Reactions as OLEDs. *Coord. Chem. Rev.* **2016**, *310*, 154−169. (b) Zhuang, J.; Li, W.; Wu, W.; Song, M.; Su, W.; Zhou, M.; Cui, Z. Homoleptic Tris-Cyclometalated Iridium(III) Complexes with Phenylimidazole Ligands for Highly Efficient Sky-Blue OLEDs. *New J. Chem.* **2015**, *39*, 246−253. (c) Ladouceur, S.; Fortin, D.; Zysman-Colman, E. Enhanced Luminescent Iridium(III) Complexes Bearing Aryltriazole Cyclometalated Ligands. *Inorg. Chem.* **2011**, *50*, 11514−11526. (d) Bolink, H. J.; De Angelis, F.; Baranoff, E.; Klein, C.; Fantacci, S.; Coronado, E.; Sessolo, M.; Kalyanasundaram, K.; Gratzel, M.; Nazeeruddin, Md. K. White-Light Phosphorescence Emission from a Single Molecule: Application to OLED. *Chem. Commun.* **2009**, 4672−4674. (e) Endo, A.; Suzuki, K.; Yoshihara, T.; Tobita, S.; Yahiro, M.; Adachi, C. Measurement of Photoluminescence Efficienty of Ir(III) Phenylpyridine Derivatives in Solution and Solid-State Films. *Chem. Phys. Lett.* **2008**, *460*, 155−157. (f) Lowry, M. S.; Bernhard, S. Synthetically Tailored Excited States: Phosphorescent, Cyclometalated Iridium(III) Complexes and Their Applications. *Chem. - Eur. J.* **2006**, *12*, 7970−7977. (g) Forrest, S. R.; Thompson, M. E.; Baldo, M. A. High-Efficiency Fluorescent Organic Light-Emitting Devices Using a Phosphorescent Sensitizer. *Nature* **2000**, *403*, 750−753. (h) Friend, R. H.; Gymer, R. W.; Holmes, A. B.; Burroughes, J. H.; Marks, R. N.; Taliani, C.; Bradley, D. D. C.; Dos Santos, D. A.; Bredas, J. L.; Logdlund, M.; Salaneck, W. R. Electroluminescence in Conjugated Polymers. *Nature* **1999**, *397*, 121−128.

(3) (a) Lo, K. K.-W.; Tso, K. K.-S. Functionalization of Cyclometalated Iridium(III) Polypyridine Complexes for the Design of Intracellular Sensors, Organelle-Targeting Imaging Reagents, and Metallodrugs. *Inorg. Chem. Front.* **2015**, *2*, 510−524. (b) Patra, M.; Gasser, G. Organometallic Compounds: an Opportunity for Chemical Biology? *ChemBioChem* **2012**, *13*, 1232−1252. (c) Baggaley, E.; Weinstein, J. A.; Williams, J. A. G. Lighting the Way to See Inside the Live Cell with Luminescent Transition Metal Complexes. *Coord. Chem. Rev.* **2012**, *256*, 1762−1785. (d) Lo, K. K.-W.; Louie, M.-W.; Zhang, K. Y. Design of Luminescent Iridium(III) and Rhenium(I) Polypyridine Complexes as in Vitro and in Vivo Ion, Molecular and Biological Probes. *Coord. Chem. Rev.* **2010**, *254*, 2603−2622. (e) Zhang, S.-J.; Hosaka, M.; Yoshihara, T.; Negishi, K.; Iida, Y.; Tobita, S.; Takeuchi, T. Phosphorescent Light-Emitting Iridium Complexes Serve as a Hypoxia-Sensing Probe for Tumor Imaging in Living Animals. *Cancer Res.* **2010**, *70*, 4490−4498. (f) Yoshihara, T.; Karasawa, Y.; Zhang, S.; Hosaka, M.; Takeuchi, T.; Iida, Y.; Endo, K.; Imamura, T.; Tobita, S. In-Vivo Phosphorescence Imaging of Cancer Using Iridium Complexes. *Proc. SPIE* **2009**, *7190*, 71900X−1. (g) Zhao, Q.; Huang, C.; Li, F. Phosphorescent Heavy-Metal Complexes for Bioimaging. *Chem. Soc. Rev.* **2011**, *40*, 2508−2524. (h) Lo, K. K.-W.; Chung, C.-K.; Lee, T. K.-M.; Lui, L.-K.; Tsang, K. H.-K.; Zhu, N. New Luminescent Cyclometalated Iridium(III) Diimine Complexes as Biological Labeling Reagents. *Inorg. Chem.* **2003**, *42*, 6886−6897.

(4) (a) Ashen-Garry, D.; Selke, M. Singlet Oxygen Generation by Cyclometalated Complexes and Applications. *Photochem. Photobiol.* **2014**, *90*, 257−274. (b) Yoshihara, T.; Yamaguchi, Y.; Hosaka, M.; Takeuchi, T.; Tobita, S. Ratiometric Molecular Sensor for Monitoring Oxygen Levels in Living Cells. *Angew. Chem., Int. Ed.* **2012**, *51*, 4148−4151. (c) Gao, R.; Ho, D. G.; Hernandez, B.; Selke, M.; Murphy, D.; Djurovich, P. I.; Thompson, M. E. Bis-Cyclometalated Ir(III) Complexes as Efficient Singlet Oxygen Sensitizers. *J. Am. Chem. Soc.* **2002**, *124*, 14828−14829.

(5) (a) Liu, Z.; Sadler, P. J. Organoiridium Complexes: Anticancer Agents and Catalysts. *Acc. Chem. Res.* **2014**, *47*, 1174−1185. (b) Geldmacher, Y.; Oleszak, M.; Sheldrick, W. S. Rhodium(III) and Iridium(III) Complexes as Anticancer Agents. *Inorg. Chim. Acta* **2012**, *393*, 84−102.

(6) (a) Huo, H.; Shen, X.; Wang, C.; Zhang, L.; Röse, P.; Chen, L.-A.; Harms, K.; Marsch, M.; Hilt, G.; Meggers, E. Asymmetric Photoredox Transition-Metal Catalysis Activated by Visible Light. *Nature* **2014**, *515*, 100−103. (b) Lalevée, J.; Tehfe, M.-A; Dumur, F.; Gigmes, D.; Blanchard, N.; Morlet-Savary, F.; Fouassier, J. P. Iridium Photocatalysts in Free Radical Photopolymerization under Visible Lights. *ACS Macro Lett.* **2012**, *1*, 286−290. (c) Goldsmith, J. I.; Hudson, W. R.; Lowry, M. S.; Anderson, T. H.; Bernhard, S. Discovery and High-throughput Screening of Heteroleptic Iridium Complexes for Photoinduced Hydrogen Production. *J. Am. Chem. Soc.* **2005**, *127*, 7502−7510.

(7) (a) Weng, J.; Mei, Q.; Jiang, W.; Fan, Q.; Tong, B.; Ling, Q.; Huang, W. Effect of pH on the Photophysical Properties of Two New Carboxylic-Substituted Iridium(III) Complexes. *Analyst* **2013**, *138*, 1689−1699. (b) Arm, K. J.; Leslie, W.; Williams, J. A. G. Synthesis and pH-Sensitive Luminescence of Bis-Terpyridyl Iridium(III) Complexes Incorporating Pendent Pyridyl Groups. *Inorg. Chim. Acta* **2006**, *359*, 1222−1232. (c) Licini, M.; Williams, J. A. G. Iridium(III) Bis-Terpyridine Complexes Displaying Long-Lived pH Sensitive Luminescence. *Chem. Commun.* **1999**, 1943−1944.

(8) For review, see: (a) Omae, I. Application of Five-membered Ring Products of Cyclometalation Reactions as Sensing Materials in Sensing Devices. *J. Organomet. Chem.* **2016**, *823*, 50−75. (b) You, Y.; Nam, W. Photofunctional Triplet Excited States of Cyclometalated Ir(III) Complexes: Beyond Electroluminescence. *Chem. Soc. Rev.* **2012**, *41*, 7061−7084. (c) Flamigni, L.; Barbieri, A.; Sabatini, C.; Ventura, B.; Barigelletti, F. Photochemistry and Photophysics of Coordination Compounds: Iridium. *Top. Curr. Chem.* **2007**, *281*, 143−203. (d) You, Y.; Park, S. Y. Phosphorescent Iridium(III) Complexes: toward High Phosphorescence Quantum Efficiency through Ligand Control. *Dalton Trans.* **2009**, 1267−1282. (e) Ulbricht, C.; Beyer, B.; Friebe, C.; Winter, A.; Schubert, U. S. Recent Developments in the Application of Phosphorescent Iridium(III) Complex Systems. *Adv. Mater.* **2009**, *21*, 4418−4441. (f) Wong, W.-Y.; Ho, C.-L. Heavy Metal Organometallic Electrophosphors Derived from Multi-Component Chromophores. *Coord. Chem. Rev.* **2009**, *253*, 1709−1758. (g) Chi, Y.; Chou, P.-T. Transition-Metal Phosphors with Cyclometalating Ligands: Fundamentals and Applications. *Chem. Soc. Rev.* **2010**, *39*, 638−655.

(9) (a) Park, G. Y.; Kim, Y.; Ha, Y. Iridium Complexes Containing Three Different Ligands as White OLED Dopants. *Mol. Cryst. Liq. Cryst.* **2006**, *462*, 179−188. (b) Felici, M.; Contreras-Carballada, P.; Smits, J. M. M.; Nolte, R. J. M.; Williams, R. M.; De Cola, L.; Feiters, M. C. Cationic Heteroleptic Cyclometalated Iridium(III) Complexes Containing Phenyl-Triazole and Triazole-Pyridine Clicked Ligands. *Molecules* **2010**, *15*, 2039−2059. (c) Edkins, R. M.; Wriglesworth, A.; Fucke, K.; Bettington, S. L.; Beeby, A. The Synthesis and Photophysics of Tris-Heteroleptic Cyclometalated Iridium Complexes. *Dalton Trans.* **2011**, *40*, 9672−9678. (d) Baranoff, E.; Curchod, B. F. E.; Frey, J.; Scopelliti, R.; Kessler, F.; Tavernelli, I.; Rothlisberger, U.; Grätzel, M.;

DOI: 10.1021/acs.inorgchem.6b02270
Inorg. Chem. XXXX, XXX, XXX−XXX

Nazeeruddin, M. K. Acid-Induced Degradation of Phosphorescent Dopants for OLEDs and its Application to the Synthesis of Tris-Heteroleptic Iridium(III) Bis-Cyclometalated Complexes. *Inorg. Chem.* **2012**, *51*, 215−224. (e) Tordera, D.; Delgado, M.; Ortí, E.; Bolink, H. J.; Frey, J.; Nazeeruddin, M. K.; Baranoff, E. Stable Green Electroluminescence from an Iridium Tris-Heteroleptic Ionic Complex. *Chem. Mater.* **2012**, *24*, 1896−1903. (f) Lepeltier, M.; Dumur, F.; Graff, B.; Xiao, P.; Gigmes, D.; Lalevée, J.; Mayer, C. R. Tris-Cyclometalated Iridium(III) Complexes with Three Different Ligands: a New Example with 2-(2,4-Difluorophenyl)pyridine-Based Complex. *Helv. Chim. Acta* **2014**, *97*, 939−956. (g) Xu, X.; Yang, X.; Wu, Y.; Zhou, G.; Wu, C.; Wong, W.-Y. Tris-Heteroleptic Cyclometalated Iridium(III) Complexes with Ambipolar or Electron Injection/Transport Features for Highly Efficient Electrophosphorescent Devices. *Chem. - Asian J.* **2015**, *10*, 252−262. (h) Lepeltier, M.; Graff, B.; Lalevée, J.; Wantz, G.; Ibrahim-Ouali, M.; Gigmes, D.; Dumur, F. Heteroleptic Iridium (III) Complexes with Three Different Ligands: Unusual Triplet Emitters for Light-Emitting Electrochemical Cells. *Org. Electron.* **2016**, *37*, 24−34.

(10) (a) Aoki, S.; Matsuo, Y.; Ogura, S.; Ohwada, H.; Hisamatsu, Y.; Moromizato, S.; Shiro, M.; Kitamura, M. Regioselective Aromatic Substitution Reactions of Cyclometalated Ir(III) Complexes: Synthesis and Photochemical Properties of Substituted Ir(III) Complexes that Exhibit Blue, Green, and Red Color Luminescence Emission. *Inorg. Chem.* **2011**, *50*, 806−818. (b) Hisamatsu, Y.; Aoki, S. Design and Synthesis of Blue-Emitting Cyclometalated Iridium(III) Complexes Based on Regioselective Functionalization. *Eur. J. Inorg. Chem.* **2011**, *2011*, 5360−5369.

(11) (a) Kando, A.; Hisamatsu, Y.; Ohwada, H.; Itoh, T.; Moromizato, S.; Kohno, M.; Aoki, S. Photochemical Properties of Red-Emitting Tris(Cyclometalated) Iridium(III) Complexes Having Basic and Nitro Groups and Application to pH Sensing and Photoinduced Cell Death. *Inorg. Chem.* **2015**, *54*, 5342−5357. (b) Hisamatsu, Y.; Shibuya, A.; Suzuki, N.; Suzuki, T.; Abe, R.; Aoki, S. Design and Synthesis of Amphiphilic and Luminescent Tris-Cyclometalated Iridium(III) Complexes Containing Cationic Peptides as Inducers and Detectors of Cell Death via a Calcium-Dependent Pathway. *Bioconjugate Chem.* **2015**, *26*, 857−879. (c) Nakagawa, A.; Hisamatsu, Y.; Moromizato, S.; Kohno, M.; Aoki, S. Synthesis and Photochemical Properties of pH Responsive Tris-Cyclometalated Iridium(III) Complexes that Contain a Pyridine Ring on the 2-Phenylpyridine Ligand. *Inorg. Chem.* **2014**, *53*, 409−422. (d) Moromizato, S.; Hisamatsu, Y.; Suzuki, T.; Matsuo, Y.; Abe, R.; Aoki, S. Design and Synthesis of a Luminescent Cyclometalated Iridium(III) Complex Having *N,N*-Diethylamino Group that Stains Acidic Intracellular Organelles and Induces Cell Death by Photoirradiation. *Inorg. Chem.* **2012**, *51*, 12697−12706. (e) Hisamatsu, Y.; Suzuki, N.; Masum, A.-A.; Shibuya, A.; Abe, R.; Sato, A.; Tanuma, S.; Aoki, S. Cationic Amphiphilic Tris-Cyclometalated Iridium(III) Complexes Induce Cancer Cell Death via Interaction with Ca^{2+}-Calmodulin Complex. *Bioconjugate Chem.* in press (DOI: 10.1021/acs.bioconjchem.6b00627).

(12) To help the readers refer to the structures of each Ir complex, the structures of all the complexes in this manuscript are listed in Chart S1 in the Supporting Information.

(13) Frisch, M. J.; Trucks, G. W.; Schlegel, H. B.; Scuseria, G. E.; Robb, M. A.; Cheeseman, J. R.; Scalmani, G.; Barone, V.; Mennucci, B.; Petersson, G. A.; Nakatsuji, H.; Caricato, M.; Li, X.; Hratchian, H. P.; Izmaylov, A. F.; Bloino, J.; Zheng, G.; Sonnenberg, J. L.; Hada, M.; Ehara, M.; Toyota, K.; Fukuda, R.; Hasegawa, J.; Ishida, M.; Nakajima, T.; Honda, Y.; Kitao, O.; Nakai, H.; Vreven, T.; Montgomery, J. A., Jr.; Peralta, J. E.; Ogliaro, F.; Bearpark, M.; Heyd, J. J.; Brothers, E.; Kudin, K. N.; Staroverov, V. N.; Kobayashi, R.; Normand, J.; Raghavachari, K.; Rendell, A.; Burant, J. C.; Iyengar, S. S.; Tomasi, J.; Cossi, M.; Rega, N.; Millam, M. J.; Klene, M.; Knox, J. E.; Cross, J. B.; Bakken, V.; Adamo, C.; Jaramillo, J.; Gomperts, R.; Stratmann, R. E.; Yazyev, O.; Austin, A. J.; Cammi, R.; Pomelli, C.; Ochterski, J. W.; Martin, R. L.; Morokuma, K.; Zakrzewski, V. G.; Voth, G. A.; Salvador, P.; Dannenberg, J. J.; Dapprich, S.; Daniels, A. D.; Farkas, Ö.; Foresman, J. B.; Ortiz, J. V.; Cioslowski, J.; Fox, D. J. *Gaussian 09*, Revision D.01; Gaussian, Inc., Wallingford CT, 2009.

(14) (a) Fantacci, S.; De Angelis, F. A Computational Approach to the Electronic and Optical Properties of Ru(II) and Ir(III) Polypyridyl Complexes: Applications to DSC, OLED and NLO. *Coord. Chem. Rev.* **2011**, *255*, 2704−2726. (b) Hay, P. J. Theoretical Studies of the Ground and Excited Electronic States in Cyclometalated Phenylpyridine Ir(III) Complexes Using Density Functional Theory. *J. Phys. Chem. A* **2002**, *106*, 1634−1641.

(15) Konno, H.; Ito, T.; Sugita, Y. Preparation of Facial Trisortho-Metalated Iridium Complexes as Light-Emitting Metals for Organic Electroluminescent Devices. PCT. Patent. WO2012/057139A1.

(16) Dumur, F.; Lepeltier, M.; Siboni, H. Z.; Gigmes, D.; Aziz, H. Phosphorescent Organic Light-Emitting Devices (PhOLEDs) Based on Heteroleptic Bis-Cyclometalated Complexes Using Acetylacetonate as the Ancillary Ligand. *Synth. Met.* **2014**, *198*, 131−136.

(17) The ^{1}H NMR spectra of **6b**, ***mer*-10**, ***fac*-12**, ***mer*-12**, ***mer*-13**, ***mer*-14**, ***mer*-15**, ***mer*-16**, **18**, **19b**, ***fac*-20**, **23b**, **24**, **25**, **26**, **28**, **29**, **30**, **31**, **35a**, **36**, and ***mer*-43** are shown in Figures S1−S22 in the Supporting Information.

(18) Agarwal, N.; Nayak, P. K. Synthesis, Characterization, Photophysical and Electrochemical Properties of New Phosphorescent Dopants for OLEDs. *Tetrahedron Lett.* **2008**, *49*, 2710−2713.

(19) Kumar, S.; Hisamatsu, Y.; Tamaki, Y.; Ishitani, O.; Aoki, S. Design and Synthesis of Heteroleptic Cyclometalated Iridium(III) Complexes Containing Quinoline-Type Ligands that Exhibit Dual Phosphorescence. *Inorg. Chem.* **2016**, *55*, 3829−3843.

(20) *Smart & SAINT Software Reference Manuals*, Version 6.45; Bruker Analytical X-ray Systems, Inc., Madison, WI, 2003.

(21) Sheldrick, G. M. *SADABS*, Software for Empirical Absorption Correction, Ver.2.05; University of Göttingen, Göttingen, Germany, 2002.

(22) *XPREP*, 5.1 ed.; Siemens Industrial Automation Inc., Madison, WI, 1995.

(23) Sheldrick, G. M. *SHELXL97*, Program for Crystal Structure Refinement; University of Göttingen, Göttingen, Germany, 2008.

(24) (a) Murov, S. L.; Carmichael, I.; Hug, G. L. *Handbook of Photochemistry*, 2nd ed.; Marcel Dekker, Inc.: New York, 1993. (b) DeBernardo, S.; Weigele, M.; Toome, V.; Manhart, K.; Leimgruber, W.; Böhlen, P.; Stein, S.; Udenfriend, S. Studies on the Reaction of Fluorescamine with Primary Amines. *Arch. Biochem. Biophys.* **1974**, *163*, 390−399.

(25) Okada, S.; Okinaka, K.; Iwawaki, H.; Furugori, M.; Hashimoto, M.; Mukaide, T.; Kamatani, J.; Igawa, S.; Tsuboyama, A.; Takiguchi, T.; Ueno, K. Substituent Effects of Iridium Complexes for Highly Efficient Red OLEDs. *Dalton Trans.* **2005**, *9*, 1583−1590.

(26) Nonoyama, M. [Benzo[h] quinolin-10-yl-N] iridium(III) Complexes. *Bull. Chem. Soc. Jpn.* **1974**, *47*, 767−768.

(27) Preparation of *fac*-heteroleptic Ir complexes by photochemical isomerization of the corresponding *mer*-isomers was reported by van Koten and co-workers. See: McDonald, A. R.; Lutz, M.; von Chrzanowski, L. S.; van Klink, G. P. M.; Spek, A. L.; van Koten, G. Probing the *mer*- to *fac*-Isomerization of Tris-Cyclometallated Homo- and Heteroleptic $(C,N)_3$ Iridium(III) Complexes. *Inorg. Chem.* **2008**, *47*, 6681−6691.

(28) (a) Deaton, J. C.; Young, R. H.; Lenhard, J. R.; Rajeswaran, M.; Huo, S. Photophysical Properties of the Series *fac*- and *mer*-(1-Phenylisoquinolinato-N∧$C^{2'}$)$_x$(2-Phenylpyridinato-N∧$C^{2'}$)$_{3-x}$iridium-(III) (x = 1−3). *Inorg. Chem.* **2010**, *49*, 9151−9161. (b) DeRosa, M. C.; Hodgson, D. J.; Enright, G. D.; Dawson, B.; Evans, C. E. B.; Crutchley, R. J. Iridium Luminophore Complexes for Unimolecular Oxygen Sensors. *J. Am. Chem. Soc.* **2004**, *126*, 7619−7626.

(29) Li, J. L. Chiral Metal Complexes as Emitters for Organic Polarized Electroluminescent Devices. PCT. Patent. WO2015/131158A1.

(30) (a) Johnson, C. K. *ORTEP: A FORTRAN Thermal-Ellipsoid Plot Program for Crystal Structure Illustrations*; Report ORNL-5138, Oak Ridge National Laboratory, Oak Ridge, TN, 1971. (b) Pennington, W. T. *DIAMOND* - Visual Crystal Structure Information System. *J. Appl.*

DOI: 10.1021/acs.inorgchem.6b02270
Inorg. Chem. XXXX, XXX, XXX−XXX

Crystallogr. **1999**, *32*, 1028−1029. (c) Cordier, G. A Versatile Tool for Displaying Crystal Structures. *Nachr. Chem., Tech. Lab.* **1999**, *47*, 1437−1438.

(31) The similar structures were reported previously. See: (a) Wong, M. Y.; Xie, G.; Tourbillon, C.; Sandroni, M.; Cordes, D. B.; Slawin, A. M. Z.; Samuel, I. D. W.; Zysman-Colman, E. Formylated Chloro-Bridged Iridium(III) Dimers as OLED Materials: Opening up New Possibilities. *Dalton Trans.* **2015**, *44*, 8419−8432. (b) Davies, D. L.; Lowe, M. P.; Ryder, K. S.; Singh, K.; Singh, S. Tuning Emission Wavelength and Redox Properties through Position of the Substituent in Iridium(III) Cyclometallated Complexes. *Dalton Trans.* **2011**, *40*, 1028−1030. (c) McGee, K. A.; Mann, K. R. Selective Low-Temperature Syntheses of Facial and Meridional Tris-Cyclometalated Iridium(III) Complexes. *Inorg. Chem.* **2007**, *46*, 7800−7809.

(32) The reaction of crude product of Entry 11 in Table 2 with acacH afforded **17** in 30% yield for 2 steps.

(33) (a) Hisamatsu, Y.; Miyazawa, Y.; Yoneda, K.; Miyauchi, M.; Zulkefeli, M.; Aoki, S. Supramolecular Complexes Formed by the Self-Assembly of Hydrophobic Bis(Zn^{2+}-Cyclen) Complexes, Copper, and Di- or Triimide Units for the Hydrolysis of Phosphate Mono- and Diesters in Two-Phase Solvent Systems (Cyclen = 1,4,7,10-Tetraazacyclododecane). *Chem. Pharm. Bull.* **2016**, *64*, 451−464. (b) Zulkefeli, M.; Hisamatsu, Y.; Suzuki, A.; Miyazawa, Y.; Shiro, M.; Aoki, S. Supramolecular Phosphatases Formed by the Self-Assembly of the Bis(Zn^{2+}-Cyclen) Complex, Copper(II), and Barbital Derivatives in Water. *Chem. - Asian J.* **2014**, *9*, 2831−2841. (c) Itoh, S.; Sonoike, S.; Kitamura, M.; Aoki, S. Design and Synthesis of Chiral Zn^{2+} Complexes Mimicking Natural Aldolases for Catalytic C-C Bond Forming Reactions in Aqueous Solution. *Int. J. Mol. Sci.* **2014**, *15*, 2087−2118. (d) Itoh, S.; Tokunaga, T.; Sonoike, S.; Kitamura, M.; Yamano, A.; Aoki, S. Asymmetric Aldol Reactions Between Acetone and Benzaldehydes Catalyzed by Chiral Zn^{2+} Complexes of Aminoacyl 1,4,7,10-Tetraazacyclododecane: Fine-Tuning of the Amino-Acid Side Chains and a Revised Reaction Mechanism. *Chem. - Asian J.* **2013**, *8*, 2125−2135. (e) Aoki, S.; Suzuki, S.; Kitamura, M.; Haino, T.; Shiro, M.; Zulkefeli, M.; Kimura, E. Molecular Recognition of Hydrocarbon Guests by a Aupramolecular Capsule Formed by the 4:4 Self-Assembly of Tris(Zn^{2+}-Cyclen) and Trithiocyanurate in Aqueous Solution. *Chem. - Asian J.* **2012**, *7*, 944−956. (f) Zulkefeli, M.; Suzuki, A.; Shiro, M.; Hisamatsu, Y.; Kimura, E.; Aoki, S. Selective Hydrolysis of Phosphate Monoester by a Supramolecular Phosphatase Formed by the Self-Assembly of a Bis(Zn^{2+}-Cyclen) Complex, Cyanuric Acid, and Copper in an Aqueous Solution (Cyclen = 1,4,7,10-Tetraazacyclododecane). *Inorg. Chem.* **2011**, *50*, 10113−10123. (g) Kitamura, M.; Suzuki, T.; Abe, R.; Ueno, T.; Aoki, S. ^{11}B NMR Sensing of d-Block Metal Ions in Vitro and in Cells Based on the Carbon-Boron Bond Cleavage of Phenylboronic Acid-Endant Cyclen (Cyclen = 1,4,7,10-Tetraazacyclododecane). *Inorg. Chem.* **2011**, *50*, 11568−11580. (h) Ohshima, R. O.; Kitamura, M.; Morita, A.; Yamada, Y.; Ikekita, M.; Kimura, E.; Aoki, S.; Shiro, M. Design and Synthesis of a Fluorescent Probe for Zn^{2+}, 5,7-Bis(*N*,*N*-Dimethylaminosulfonyl)-8-Hydroxyquinoline-Pendant 1,4,7,10-Tetraazacyclododecane and Zn^{2+}-Dependent Hydrolytic and Zn^{2+}-Independent Photochemical Reactivation of Its Benzenesulfonyl-Caged Derivative. *Inorg. Chem.* **2010**, *49*, 888−899.

(34) For review, see: (a) Kimura, E.; Koike, T.; Aoki, S. in *Macrocyclic and Supramolecular Chemistry: How Izatt-Christensen Award Winners Shaped the Field*; Izatt, R. M., Ed.; John Wiley & Sons, Ltd.: NJ, 2016; pp 417−445. (b) Aoki, S.; Ariyasu, S.; Hanaya, K.; Hisamatsu, Y.; Sugai, T. Chemical Reactions of 8-Quinolinol Derivatives and Their Applications to Biochemical Tools and Enzyme Inhibitors. *Yuki Gosei Kagaku Kyokaishi* **2016**, *74*, 482−493. (c) Aoki, S.; Zulkefeli, M.; Kitamura, M.; Hisamatsu, Y. in *Synergy in Supramolecular Chemistry*; Nabeshima, T., Ed.; CRC: Boca Raton, FL, 2015; pp 35−56. (d) Kimura, E. Evolution of Macrocyclic Polyamines from Molecular Science to Supramolecular Science. *Bull. Jpn. Soc. Coord. Chem.* **2012**, *59*, 26−47. (e) Aoki, S.; Kimura, E. Zinc-Nucleic Acid Interaction. *Chem. Rev.* **2004**, *104*, 769−787.

(35) The crude product of the BF_3-promoted decomposition reaction (Entry 20 of Table 2) was directly reacted with acacH to give **17** in 19% (2 steps), suggesting that the $BF_3{\cdot}Et_2O$-promoted decomposition of ***fac*-2** affords the uncharacterized intermediate, not **6a**, which reacts with acacH to give **17** in a low yield.

(36) The ^1H NMR signals of **27a** and **27b** in the lowest magnetic field were assigned to be hydrogen atoms on carbon next to the nitrogen (Figure S24 in the Supporting Information). The left peaks of **27b** (at δ = ca. 9.5) exhibit a greater downfield shift than **27a** (at δ = ca. 9.2), inidicating that the shielding effect of bromine atom is weaker than that of chlorine atom.

(37) It should be mentioned that the decomposition of ***fac*-12** requires longer reaction time than that of ***mer*-12** (Entry 1 vs Entry 2 in Table 6), possibly because ***fac*-12** is more stable by ca. 26 kJ/mol than ***mer*-12**, as calculated by DFT calculation (the difference in total energies of ***fac*-12** and ***mer*-12** is 0.01 au, which corresponds to ca. 26 kJ/mol, as indicated in Table S1 in the Supporting Information).

(38) Dual emitting Ir complexes have been reported as useful phosphorescent materials and bioimaging probes. See: (a) Zhang, K. Y.; Liu, H.-W.; Tang, M.-C.; Choi, A. W.-T.; Zhu, N.; Wei, X.-G.; Lau, K.-C.; Lo, K. K.-W. Dual-Emissive Cyclometalated Iridium(III) Polypyridine Complexes as Ratiometric Biological Probes and Organelle-Selective Bioimaging Reagents. *Inorg. Chem.* **2015**, *54*, 6582−6593. (b) Ladouceur, S.; Donato, L.; Romain, M.; Mudraboyina, B. P.; Johansen, M. B.; Wisner, J. A.; Zysman-Colman, E. A Rare Case of Dual Emission in a Neutral Heteroleptic Iridium(III) Complex. *Dalton Trans.* **2013**, *42*, 8838−8847. (c) You, Y.; Han, Y.; Lee, Y.-M.; Park, S. Y.; Nam, W.; Lippard, S. J. Phosphorescent Sensor for Robust Quantification of Copper(II) Ion. *J. Am. Chem. Soc.* **2011**, *133*, 11488−11491. (d) You, Y.; Lee, S.; Kim, T.; Ohkubo, K.; Chae, W.-S.; Fukuzumi, S.; Nam, W.; Lippard, S. J.; Jhon, G.-J. Phosphorescent Sensor for Biological Mobile Zinc. *J. Am. Chem. Soc.* **2011**, *133*, 18328−18342. (e) Lo, K. K.-W.; Zhang, K. Y.; Leung, S.-K.; Tang, M.-C. Exploitation of the Dual-Emissive Properties of Cyclometalated Iridium(III)-polypyridine Complexes in the Development of Luminescent Biological Probes. *Angew. Chem., Int. Ed.* **2008**, *47*, 2213−2216. (f) Lee, Y. H.; Park, G. Y.; Kim, Y. S. White Light Emission Using Heteroleptic Tris-Cyclometalated Iridium(III) Complexes. *J. Korean Phys. Soc.* **2007**, *50*, 1722−1728. (g) Yeh, Y.-S.; Cheng, Y.-M.; Chou, P.-T.; Lee, G.; Yang, C.-H.; Chi, Y.; Shu, C.-F.; Wang, C.-H. A New Family of Homoleptic Ir(III) Complexes: Tris-Pyridyl Azolate Derivatives with Dual Phosphorescence. *ChemPhysChem* **2006**, *7*, 2294−2297.

(39) Baranoff and co-workers reported the X-ray structure analysis of Ir(ppy)(F_2ppy) (acac) having two pyridines of its ppy and F_2ppy ligands in *trans* positions to each other (ref 9d), which is similar to the structure of **35a**.

(40) We have recently reported on the design and synthesis of tris-heteroleptic cyclometalated Ir complexes consisting of three different non-symmetric ligands based on ligand-selective electrophilic reactions. See Hisamatsu, Y.; Kumar, S.; Aoki, S. Design and Synthesis of Tris-Heteroleptic Cyclometalated Iridium(III) Complexes Consisting of Three Different Nonsymmetric Ligands Based on Ligand-Selective Electrophilic Reactions via Interligand HOMO Hopping Phenomena. *Inorg. Chem.* in press (DOI: 10.1021/acs.inorgchem.6b02519).

(41) (a) Atkins, P.; Overton, T.; Rourke, J.; Weller, M.; Armstrong, F. *Inorganic Chemistry*, 4th ed.; Oxford University Press, Oxford, U. K., 2006. (b) Pearson, R. G. Hard and Soft Acids and Bases. *J. Am. Chem. Soc.* **1963**, *85*, 3533−3539.

(42) Zhou, B.; Hu, Y.; Wang, C. Manganase-Catalyzed Direct Nucleophilic C(sp^2)-H Addition to Aldehydes and Nitriles. *Angew. Chem., Int. Ed.* **2015**, *54*, 13659−13663.

(43) It is described that ligands functionalized with NO_2 and Br groups stabilize metal complexes. See: Lima, C. F. R. A. C.; Taveira, R. J. S.; Costa, J. C. S.; Fernandes, A. M.; Melo, A.; Silva, A. M.; Santos, L. M. N. B. F. Understanding M−Ligand Bonding and *mer*-/*fac*-Isomerism in Tris(8-Hydroxyquinolinate) Metallic Complexes. *Phys. Chem. Chem. Phys.* **2016**, *18*, 16555−16565.

DOI: 10.1021/acs.inorgchem.6b02270
Inorg. Chem. XXXX, XXX, XXX−XXX

(44) Housecroft, C. E.; Sharp, A. G. *Inorganic Chemistry*, 4th ed.; Pearson Education Ltd.: London, 2012.
(45) Uneyama, K.; Katagiri, T.; Amii, H. α−Trifluoromethylated Carbanion Synthons. *Acc. Chem. Res.* **2008**, *41*, 817−829.
(46) The Ir-C and Ir-N bond lengths obtained by our DFT calculations of the *fac*- and *mer*-forms of **1**, **2**, **8**, and **10** are nearly identical to the values reported by Thompson and co-workers (ref 1h; see Table S1 in the Supporting Informtion).
(47) As shown in Figure S31 in the Supporting Information, the emission maxima of ***fac*-12** (516 nm) is 12 nm shorter than that of the ***mer*-12** and the luminescent quantum yield of ***fac*-12** (Φ = 0.57) is nearly ten times higher than that ***mer*-12** ($\Phi = 4.7 \times 10^{-2}$). It should be noted that Thompson and co-workers reported that *fac*-form of tris-cyclometalated homoleptic Ir complexes exhibit higher emission quantum yield than the corresponding *mer*-complexes (e.g.; ***fac*-2** and ***mer*-2**) (ref 1h). The emission lifetime of ***fac*-12** (τ = 1.9 μs) is longer than that for ***mer*-12** (τ = 0.3 μs). The slightly shorter emission wavelength of ***mer*-13** (504 nm) compared to ***mer*-12** can be attributed to the electron-withdrawing effect of the fluorine atom. The quantum yield and emission lifetimes of ***mer*-14** are both small ($\Phi = 8.3 \times 10^{-2}$, τ = 0.25 μs) and the emission maxima is 512 nm. Interestingly, the emission maxima of ***mer*-16** (581 nm) is somewhat shorter than that of ***mer*-15** (603 nm) and its Φ value and emission lifetime (Φ = 0.31, τ = 4.7 μs) are greater than those of ***mer*-15** (Φ = 0.22, τ = 1.1 μs).

DOI: 10.1021/acs.inorgchem.6b02270
Inorg. Chem. XXXX, XXX, XXX−XXX